NASA/TM-20210014627

Lunar Equator Regenerative Fuel Cell System Efficiency Analysis

Phillip J. Smith, Kerrigan P. Cain, Ryan P. Gilligan, and Ian J. Jakupca
Glenn Research Center, Cleveland, Ohio

August 2022

NASA STI Program . . . in Profile

Since its founding, NASA has been dedicated to the advancement of aeronautics and space science. The NASA Scientific and Technical Information (STI) Program plays a key part in helping NASA maintain this important role.

The NASA STI Program operates under the auspices of the Agency Chief Information Officer. It collects, organizes, provides for archiving, and disseminates NASA's STI. The NASA STI Program provides access to the NASA Technical Report Server—Registered (NTRS Reg) and NASA Technical Report Server—Public (NTRS) thus providing one of the largest collections of aeronautical and space science STI in the world. Results are published in both non-NASA channels and by NASA in the NASA STI Report Series, which includes the following report types:

- TECHNICAL PUBLICATION. Reports of completed research or a major significant phase of research that present the results of NASA programs and include extensive data or theoretical analysis. Includes compilations of significant scientific and technical data and information deemed to be of continuing reference value. NASA counter-part of peer-reviewed formal professional papers, but has less stringent limitations on manuscript length and extent of graphic presentations.

- TECHNICAL MEMORANDUM. Scientific and technical findings that are preliminary or of specialized interest, e.g., "quick-release" reports, working papers, and bibliographies that contain minimal annotation. Does not contain extensive analysis.

- CONTRACTOR REPORT. Scientific and technical findings by NASA-sponsored contractors and grantees.

- CONFERENCE PUBLICATION. Collected papers from scientific and technical conferences, symposia, seminars, or other meetings sponsored or co-sponsored by NASA.

- SPECIAL PUBLICATION. Scientific, technical, or historical information from NASA programs, projects, and missions, often concerned with subjects having substantial public interest.

- TECHNICAL TRANSLATION. English-language translations of foreign scientific and technical material pertinent to NASA's mission.

For more information about the NASA STI program, see the following:

- Access the NASA STI program home page at http://www.sti.nasa.gov

- E-mail your question to help@sti.nasa.gov

- Fax your question to the NASA STI Information Desk at 757-864-6500

- Telephone the NASA STI Information Desk at 757-864-9658

- Write to:
  NASA STI Program
  Mail Stop 148
  NASA Langley Research Center
  Hampton, VA 23681-2199

NASA/TM-20210014627

Lunar Equator Regenerative Fuel Cell System Efficiency Analysis

Phillip J. Smith, Kerrigan P. Cain, Ryan P. Gilligan, and Ian J. Jakupca
Glenn Research Center, Cleveland, Ohio

National Aeronautics and
Space Administration

Glenn Research Center
Cleveland, Ohio 44135

August 2022

Acknowledgments

The authors would like to thank Wesley Johnson for supporting the liquefaction calculations, Francis Davies for input on voltage regulation, William Bennett and Jessica Cashman for review of the manuscript, and Frederick Elliot and Mathew Deminico for their project leadership.

Level of Review: This material has been technically reviewed by technical management.

Lunar Equator Regenerative Fuel Cell System Efficiency Analysis

Phillip J. Smith, Kerrigan P. Cain, Ryan P. Gilligan, and Ian J. Jakupca
National Aeronautics and Space Administration
Glenn Research Center
Cleveland, Ohio 44135

Summary

It is expected that future NASA mission energy storage requirements can be adequately met by regenerative fuel cells (RFCs). Aerospace RFCs are likely to package proton exchange membrane electrochemical conversion devices based on hydrogen, oxygen, and water. To optimize system designs and direct further development, the most useful system metric is round-trip efficiency (RTE). Improving RTE generally increases specific energy and reduces system mass. The following analysis models the impact of several factors on RTE for RFCs scaling from 0.1 to 50 kW. The analysis demonstrates that higher electrolyzer (EZ) operational pressure most negatively impacts both RFC RTE and specific energy. Reactant storage heating and power management losses are significant for RFCs of any scale, but solenoid valve power becomes a noticeable parasitic load for smaller RFCs. Spherical gas storage vessels benefit RTE by only 2 to 4 percentage points but increase specific energy by ~50 percent. Cryogenic reactant storage is shown to depress RTE to below 15 percent in all cases. For a given RFC scale, there is an RTE benefit to specifying larger EZs and recharging at higher rates—if the RFC can be coupled with a corresponding power source. Although fuel cell (FC) operation is less impactful on RTE than EZ factors, efficiency is maximized by sizing the FCs relatively large and keeping current density low. RFC design is a balance of many interrelated factors, but this analysis provides a starting point for difficult decisions that must be made when designing a lunar equator RFC.

Acronyms

BoP balance-of-plant
EZ electrolyzer
FC fuel cell
PEM proton exchange membrane
PMAD power management and distribution
PV photovoltaic
RFC regenerative fuel cell
RTE round-trip efficiency

1.0 Introduction

NASA anticipates sending robotic payloads to the Moon starting in the early 2020s and eventually establishing a human presence by the late 2020s. Long-term lunar missions require energy storage systems capable of providing electrical power during times of sunlight and eclipse. For most space missions with access to sunlight and comparatively low energy demands, photovoltaic (PV) systems convert sunlight into electricity and are typically coupled with an energy storage system such as a battery. Because of the long eclipse periods encountered on the Moon, the very high energy requirements render battery storage systems prohibitively massive and impractical for extended duration surface-operation missions. Although nuclear power systems operate independently of sunlight and are a viable lunar application power source, regulatory concerns and oversight significantly increase the required resources

to implement nuclear power systems. Regenerative fuel cells (RFCs) offer a feasible solution to meet the energy storage needs of NASA lunar surface payloads from landers to rovers and stationary power systems.

An RFC consists of a fuel cell (FC) and an electrolyzer (EZ) combined with a reactant storage system. FCs are energy conversion devices that convert chemical potential energy into electrical energy. Proton exchange membrane (PEM) FCs consume hydrogen and oxygen gas to produce electricity, heat, and water. EZs produce hydrogen and oxygen gas by splitting water when supplied with electricity. RFCs must couple with a suitable external power supply, such as PV arrays, to provide power when the FC is not operating. All nonnuclear options will be comparatively high mass (Ref. 1), but RFCs are desirable for missions that cannot afford nuclear power or accommodate it because of regulatory issues.

Of all system-level performance metrics, round-trip efficiency (RTE) is potentially the most useful in evaluation. Theoretical maximum RTE is ~80 percent, comparable to batteries, but specific energy is potentially higher for RFCs (Ref. 2). Improving efficiency is often secondary to reducing mass in flight systems (Ref. 3), but the two are not completely separate entities in RFC design. A past RFC design study noted conflicting design criteria in that highest efficiency comes from highest temperature, low pressure, and lowest current density; lowest mass comes from highest temperature, lowest pressure, and highest current density; best reliability comes from minimizing all three of those categories (Ref. 4). This makes it difficult to optimize an RFC for both RTE and mass in all scenarios.

Still, at any level, an efficiency improvement produces corresponding benefits elsewhere in the system. For example, reduced parasitic power consumption results in less reactant that must be stored and regenerated. As a result, the storage vessels could be smaller, have lower mass, and require less thermal power during a lunar night. In addition, the electrochemical stacks could be reduced in size or able to operate at a more efficient and reliable level. Smaller or more efficient stacks would generate less waste heat, corresponding to lower coolant flow rates and smaller radiators. Furthermore, less power would be transferred in and out of the boundary separating the energy storage system from the initial power source or end power user (hereafter, referred to as “customer”), thus reducing both absolute voltage conversion losses and solar array size.

It has been suggested that EZ and FC stack and reactant storage improvements should be the focus for further improving RTE and specific energy (Ref. 2). Regardless of where the initial efficiency improvement originates (e.g., electrochemical stacks, fluidic components, or other hardware), the described circular, cascading effects occur in every case. This RFC efficiency analysis is intended to inform potential flight system designers on the major factors affecting round-trip energy efficiency. As a result, a common ground will be established for comprehending these elements and what can realistically be accomplished to optimize RFCs for flight utilization.

The presented results incorporate electrochemical, fluidic, power management and distribution (PMAD), and thermal considerations for RFC operation in a lunar equator environment based on conditions near the Murchison Crater. The chosen location represents a worst-case for RFCs, at least among lunar locations and especially at lower power levels. NASA has studied (Ref. 5) and modeled RFCs for many decades (Refs. 4 and 6), though many of these reports focused on a single nominal power level, short cycle times for space station application (Ref. 7), alkaline-based electrochemical stacks (Refs. 4 and 8), or lunar south pole locations (Refs. 1, 8, and 9). RFCs have been identified as desirable options for applications as disparate as small-scale landers (Ref. 10), 2-kW rovers (Ref. 1), and beyond 20 to 40 kW for bases (Refs. 6, 11, and 12). It is desirable to have a single study that evaluates a range of RFC power scales, optimizing for each level to evaluate what is possible rather than simply assuming modularity and adding complete units together.

Building on more recent NASA trade studies (Refs. 12 to 16), the assumed RFC system architecture is based on utilization of hydrogen-oxygen PEM technology for both the discrete FC and EZ stacks. Although there have been evaluations of unitized RFC concepts (Ref. 17), PEM stacks of this type are still not advanced enough for flight consideration. There is minimal mass and volume reduction achieved by the unitized concept for long-duration missions, and discrete stacks enable optimization of stack sizing to improve efficiency in scenarios where charge and discharge power levels are different (Ref. 2). Barbir (Ref. 2) found no distinct advantage to either concept, but the discrete RFC had higher potential efficiency (RTE maximum of 38 percent for a discrete RFC and 35 percent for unitized RFC, both inclusive of parasitic loads), possibly providing more benefit in reducing the masses of gas storage and the solar array (Ref. 2). When assuming short 12-h charge and 12-h discharge periods as Barbir did, there is worthwhile debate on which style of RFC to choose. For a longer duration lunar cycle, optimizing efficiency and focusing on reactant storage masses becomes much more critical. In References 7 and 18, discrete RFCs were baselined over unitized because of expected lower development cost, likely easier maintenance, and better ability to optimize design—all of which are still likely true today.

The purpose of this analysis is not to cover all factors that influence RTE. Nearly every RFC design decision may be critical for optimizing RTE, depending on mission concept. For a lunar equator application, multiple significant design decisions are discussed and compared to previously modeled and demonstrated results. These factors include (1) EZ decisions, such as active area, membrane thickness, operational pressure and temperature, and power profile; (2) FC decisions, such as active area and current density design point; (3) component decisions, such as solenoid valve operation and type and voltage converters; and (4) reactant storage decisions, such as vessel configuration, gas versus cryogenic storage, and storage vessel temperature.

2.0 Approach

Figure 1 shows the primary subsections and interconnections that form the RFC system for this analysis. The FC is a non-flow-through design that incorporates passive internal water separation. The EZ is a liquid-anode-feed unit requiring external water separation for both hydrogen and oxygen product gases. The fluidic balance-of-plant (BoP) consists of all storage vessels, valves, regulators, heaters, pumps, and sensors required to supply and store hydrogen, oxygen, water, and coolant, as needed. The PMAD subsystem includes voltage converters required for internal power management and integration with a customer. Reported system metrics do not include solar array physical sizing estimates, but solar array considerations are discussed as part of the EZ design.

A nominal 0.1-kW RFC is modeled as a baseline case. Model input assumptions are listed in the Appendix. This system is designed to support the FC net power load profile shown in Figure 2. This profile equates to an average net power of 106 W with peaks of up to 400 W. Net power is the electricity provided to a customer whereas gross power includes all internal parasitic loads that the FC must supply. RFC gross input power, or charge power, includes all parasitic loads during EZ operation in addition to the power required to split water. RFC RTE is a function of the net energy produced during lunar night phases and the gross input energy.

A 0.1-kW-class RFC is among the lowest power levels practical for an RFC. Even with the long lunar night durations, the comparative performance and simplicity of batteries are appealing at 0.1 kW or less power levels. As such, this scale is not ideal for highlighting the specific energy potential of RFCs. Still, it aligns with existing NASA projects and is a useful case study to discuss relative impacts of system design selections while representing an energy storage option that would not be out of place in a suitable midsize lander.

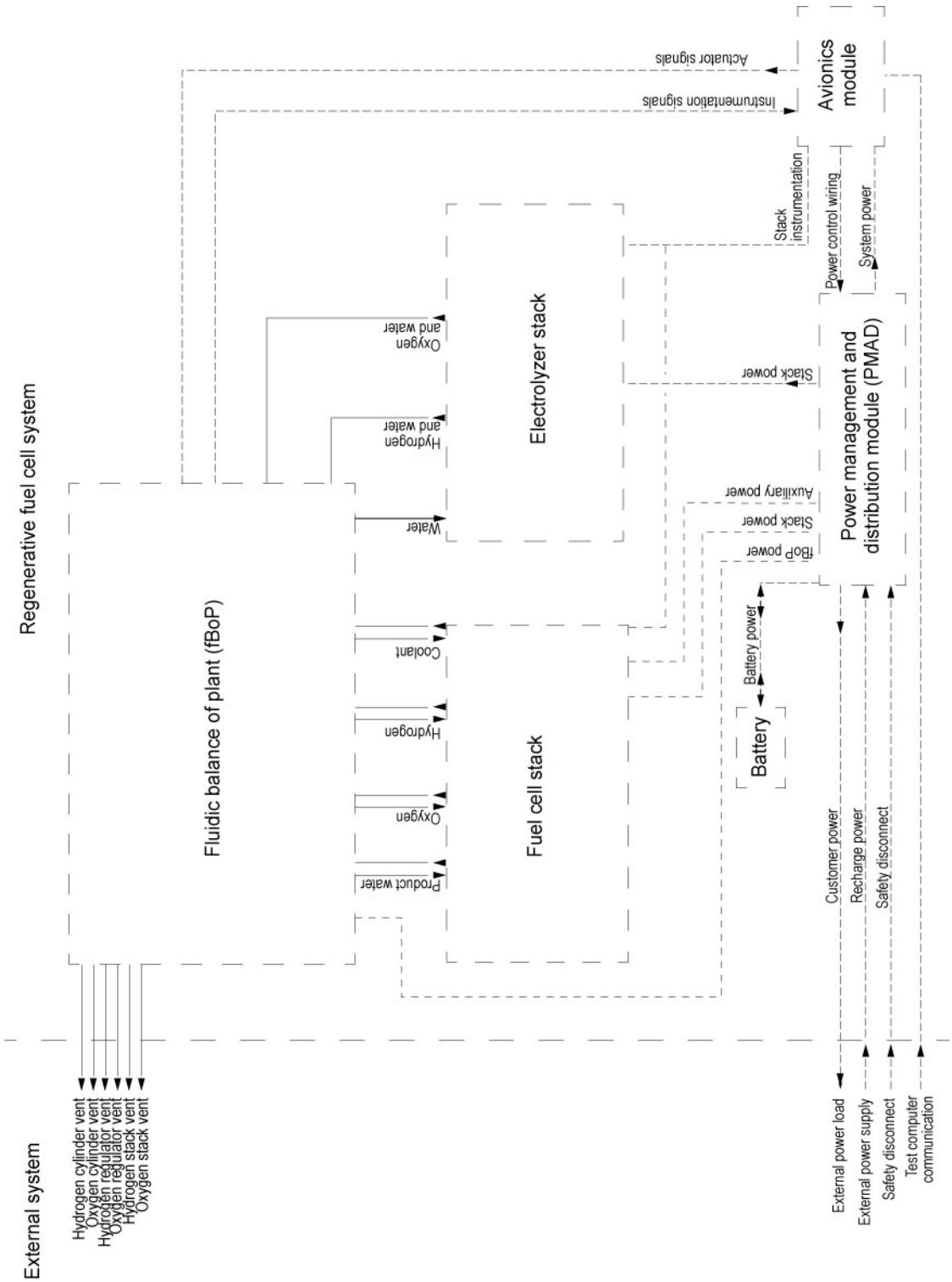

Figure 1.—Regenerative fuel cell system primary subsections and connections.

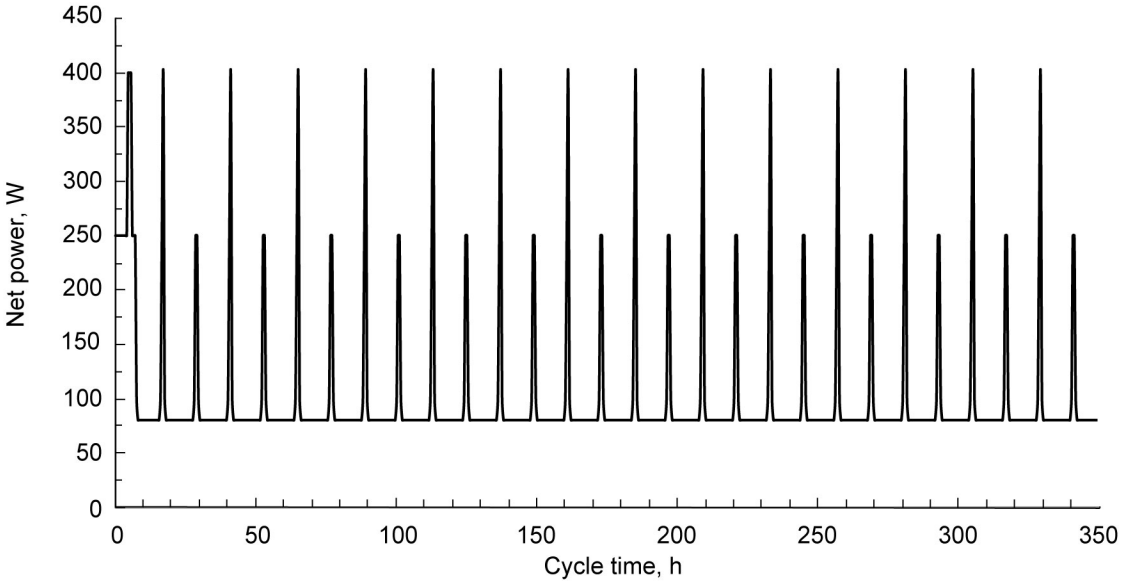

Figure 2.—Fuel cell net power load profile.

Other RFCs are modeled assuming constant required nominal net power outputs of 0.1, 0.25, 0.5, 1, 5, 10, 25, and 50 kW. No variable profile was simulated for any of these cases, but given the conservative FC stack sizing, it is realistic to produce maximum net power outputs of at least 4 times the nominal net power. Extended duration operation in such a condition would affect the absolute values of the reported system metrics and would increase required reactant storage mass. Fuel cell output is constant throughout the lunar night, tapers off in the morning, and gradually increases towards the end of the lunar day to support variable solar array output.

Any reported system metrics, such as specific energy, are for comparison purposes only and not to be accepted as absolute values without context. The modeled systems are designed to function in assumed-worst-case scenarios, defined as being a lunar cycle with the lowest available total solar energy. For comparison, a best case, representing a lunar cycle with the greatest available total solar energy, may also be presented. Unless otherwise noted, all modeled systems are designed to store enough energy to satisfy worst-case conditions without any power production compromises. No accommodation is made for any redundancy. No reported cases herein necessarily represent the absolute best-case results for any particular scenario. Mission risk tolerance (i.e., the need for redundancy and de-rating); exact mission location; other design constraints on mass, volume, or particular dimensions; and electrical requirements all make it difficult to speculate on practical limits for efficiency.

3.0 Results

3.1 Reactant Mass Change Due to RTE

Table I shows the effect of RFC RTE on required reactant mass. The baseline values represent the current model scenario based on anticipated NASA requirements and preliminary electrochemical stack performance estimates for the baseline 0.1-kW RFC case. Improving RTE by 1 percentage point reduces the reactant mass by 2.9 percent. This reduction has carryover effects in that storage vessel mass and parasitic loads also decrease in magnitude. The absolute numbers are small for a 0.1-kW-scale system, but this translates to a decrease in mass by several hundred kilograms in a 10-kW system.

TABLE I.—ROUND-TRIP EFFICIENCY EFFECT ON RFC REQUIRED REACTANT MASS

Efficiency change, percentage points	Mass, kg			Mass change, percent
	Hydrogen	Oxygen	Total	
–2	5.7	42.8	48.5	6.6
–1	5.5	41.3	46.8	2.8
Baseline	5.4	40.1	45.5	0.0
1	5.2	39.0	44.2	–2.9
2	5.1	37.7	42.8	–6.1

TABLE II.—PARASITIC LOADS DURING RFC FUEL CELL OPERATION FOR THREE POWER PROFILES

Component	Power consumption, W		
	0.1-kW baseline	1-kW constant	50-kW constant
Gas storage heater power	83	180	2,000
Solenoid valves	36	70	230
Power management and distribution (PMAD)	23	50	2,500
Coolant pump	4	45	1,700
Product water degassing	1	10	100

3.2 Parasitic Load Rankings

3.2.1 Parasitic Loads During Fuel Cell Operation

There are two primary phases of RFC operation: when the FC provides system power and when the EZ consumes system power. Different sets of BoP components are operating during these two phases. The nominal FC parasitic loads are listed in Table II for three RFC scales. One of the largest losses is from heating the reactant storage vessels, which are located outside of the thermal enclosure. In multi-kilowatt-class RFCs, reactant storage constitutes the majority of the mass and volume of the entire system. Even though it is not unreasonable to design a single thermal enclosure to contain a complete 0.1-kW-class RFC system that includes reactant storage, this does not scale up satisfactorily. If hydrogen and oxygen can be adequately separated from water after exiting the EZ, there is no need for the gases to be maintained in the relatively narrow thermal environment required by water-containing components. This is a current unknown in RFC design, and results shown here assume storage vessels are maintained above 4 °C, which is an impactful decision. For the 0.1-kW baseline RFC, instead of the 83 W required to keep the vessels above 4 °C, only 37 W are needed to maintain the vessels above –50 °C during the lunar night. Still, heating is a noticeable parasitic load that is necessary to avoid oxygen liquefaction and meet the FC minimum reactant supply temperature. For more discussion on this issue, refer to Section 3.6.3, Reactant Storage Temperature.

Without incorporation of spike-and-hold or latching valve concepts (see Sec. 3.5.2), solenoid valves are likely to be one of the largest periodic parasitic loads during FC operation for small RFCs. Although the baseline system is a 0.1-kW-nominal RFC, it is capable of delivering more power for durations of several hours. During high power production periods when a customer is receiving up to 400 W of

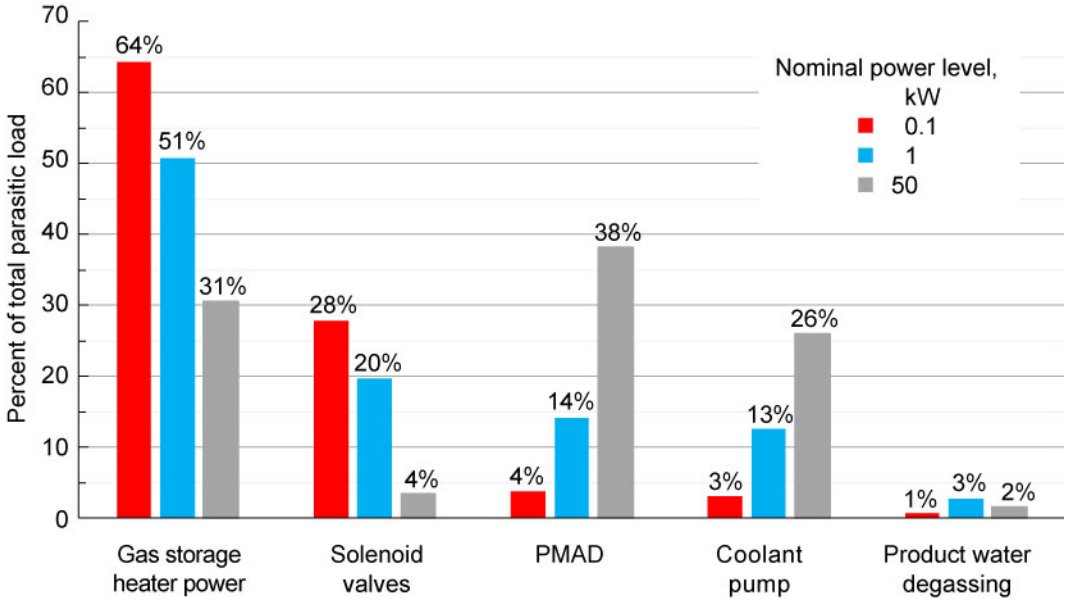

Figure 3.—Percentage of each nominal parasitic load relative to parasitic load total during fuel cell operation for regenerative fuel cells at 0.1, 1, and 50 kW nominal power levels.

electrical power, PMAD losses (assuming 95 percent voltage conversion efficiency) approach the solenoid total, though average PMAD losses are much less.

The remaining parasitic loads are smaller in magnitude. There is a continuously operating coolant pump to provide flow through the FC, heat exchangers for PMAD components, the EZ, and radiator. FC product water is likely to contain dissolved oxygen gas. Therefore, product water degassing is accomplished in a FC stack auxiliary cell, and this places a small load on the rest of the stack.

Figure 3 shows that PMAD losses become the primary parasitic load as RFC nominal power output increases. There is no size benefit to these components with increases in RFC power output, and the power loss simply scales with RFC power output. Coolant pump power also nearly scales with RFC power level, but it becomes a greater fraction of the total parasitic load at larger scales. Gas storage vessel heating is still significant, as it is the second largest parasitic load at 50 kW, but much less impactful on the RTE. This is likely due to the better volume-to-surface-area ratios that are achievable with larger vessels. Such a benefit may not be observed if larger storage volumes are obtained simply through multiple smaller vessels. Regardless of the RFC scale, the required quantity of solenoid valves is unlikely to change, so although larger valves tend to consume more power, it is a minor increase in comparison to RFC scale.

3.2.2 Parasitic Loads During Electrolyzer Operation

The average and maximum EZ parasitic loads are listed in Table III for multiple RFC scales. Note that the nominal power levels represent the RFC net power output and not the EZ charge rate. Because of RFC inefficiencies and the load profile required at a lunar equatorial location, electrolysis must proceed at a higher rate relative to the FC. Maximum electrical input power to the EZ is more than double the maximum power produced by the FC. Correspondingly, voltage converter inefficiency (again assuming 95 percent voltage conversion efficiency) leads to increased PMAD losses. There are fewer solenoid valves in continuous operation during electrolysis mode compared with FC mode, resulting in lower power consumption. The current RFC design includes continuous circulation from the coolant pump and two pumps for pressurizing then recirculating water to supply and cool the EZ stack.

TABLE III.—PARASITIC LOADS DURING RFC ELECTROLYZER OPERATION FOR THREE POWER PROFILES

Component	Power consumption, W					
	0.1-kW baseline		1-kW constant		50-kW constant	
	Average[a]	Maximum[b]	Average[a]	Maximum[b]	Average[a]	Maximum[b]
Power management and distribution (PMAD)	50	100	240	400	10,000	15,000
Solenoid valves	27	49	40	80	50	100
High-pressure pump	5	5	60	60	1,200	1,900
Coolant pump	4	4	45	45	1,700	1,700

[a]Average value across entire electrolyzer (EZ) operating duration.

[b]Peak value occurring anytime during EZ operating duration.

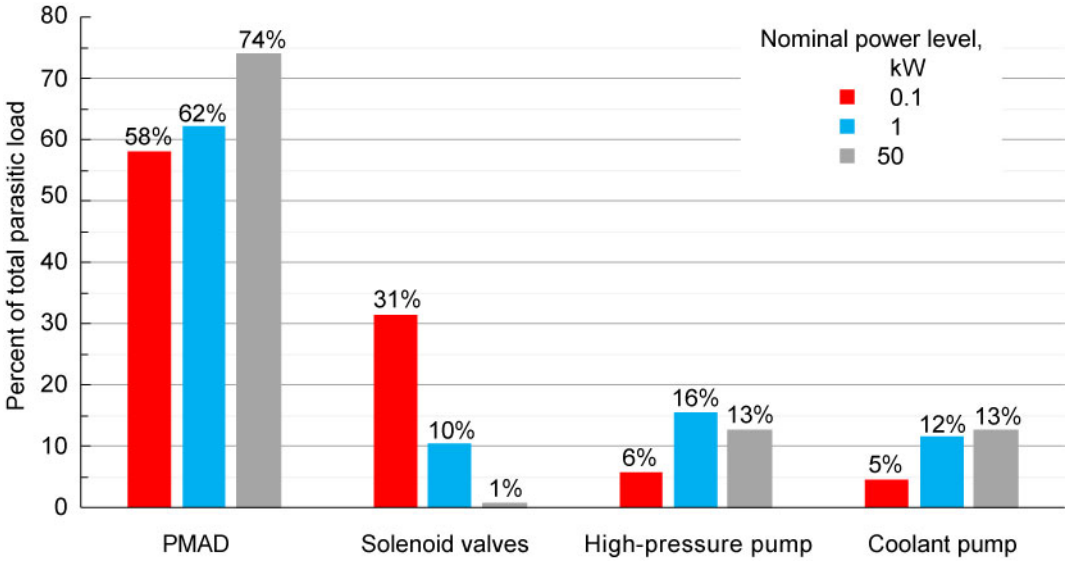

Figure 4.—Percentage of each average parasitic load relative to parasitic load total during electrolyzer operation for regenerative fuel cells at 0.1, 1, and 50 kW nominal power levels.

During EZ operation, PMAD remains the most significant loss at the larger RFC scale, as shown in Figure 4. RFC charge power is always a multiple of the net power output, thus a need for voltage regulation on the input side is going to generate notable losses. Whereas coolant pump power is nearly proportional to RFC net power and there is a small power increase for larger solenoid valves, the scale-up of the high-pressure EZ water feed pump becomes the second largest load. Some RFC models assume isothermal compression for pressurizing feed to the EZ stack (Ref. 2). This is not necessarily a realistic assumption because of real-world inefficiencies (Ref. 19). Although there are pumps in development that attempt to approach this condition (Ref. 20), the model employed in this report bases component specifications on existing commercially available products, when available. This is why the parasitic load estimation for certain components does not scale precisely linearly with RFC scale. Although there are many existing solenoid valves that could suitably function for RFCs, there are very few adequate high-pressure water pumps. Thus, there may be conditions in the model where a component such as a pump is oversized and inefficient for a given scale.

3.3 Electrolyzer Considerations

3.3.1 Reactant Storage Pressure

In RFCs with short cycle durations, on the order of hours, reactant storage mass may be only about 25 percent of the total system mass (Ref. 21). Even in the 0.1-kW lunar equator cases here, reactant storage is ~65 percent of the total RFC mass. Therefore, reactant storage is impactful to lunar equator RFC system metrics. The most important reactant storage design decision is the storage pressure. In the absence of additional compressors, EZ operational pressure effectively determines reactant storage pressure. In studying alkaline RFCs, Chang assumed pressure effects on stack performance to be negligible between 0.93 and 3.90 MPa (135 and 565 psia) (Ref. 4). A practical PEM system is likely to store gases at higher pressure. The general design principle is to operate at the highest pressure that still allows for an acceptable RTE (Ref. 18).

In Figure 5 and Figure 6, RFC net specific energy and RTE, respectively, are presented for EZ operation at 3.45, 10.34, 13.79, 17.24, and 27.58 MPa (500, 1,500, 2,000, 2,500, and 4,000 psia). For all RFC power output levels, there is minimal difference in specific energy for storage pressures ranging from 10.34 to 17.24 MPa (1,500 to 2,500 psia), with a slight benefit as pressure decreases. Reactant storage at 27.58 MPa (4,000 psia) results in the lowest specific energy for all calculated power levels. For RFCs smaller than 1 kW, 3.45 MPa (500 psia) storage is worse than the 10.34 to 17.24 MPa (1,500 to 2,500 psia) cases, but there is a benefit at 10 kW and greater.

Operation at higher pressure increases the mass of the gas storage vessels, EZ stack hardware, and BoP components in order to generate and isolate the greater pressures. This tends to penalize the resulting specific energy value at all levels, though there is also a penalty to low-pressure operation at small scales. At 0.1 kW, the storage vessels alone, excluding reactant, are 25 percent heavier at 3.45 MPa (500 psia) than at 10.34 MPa (1,500 psia) since the increase in vessel size dwarfs the benefit of thinner walls. It is notable that this trend is observed even though modeled hydrogen storage densities by mass (i.e., hydrogen mass divided by the total of hydrogen mass and storage vessel mass) are quite high. It has been reported that 5 to 10 percent reactant storage densities are achievable for hydrogen (Ref. 2), and ~9 percent at 27.58 MPa (4,000 psia) to ~11 percent at 3.45 MPa (500 psia) are the results for cases here.

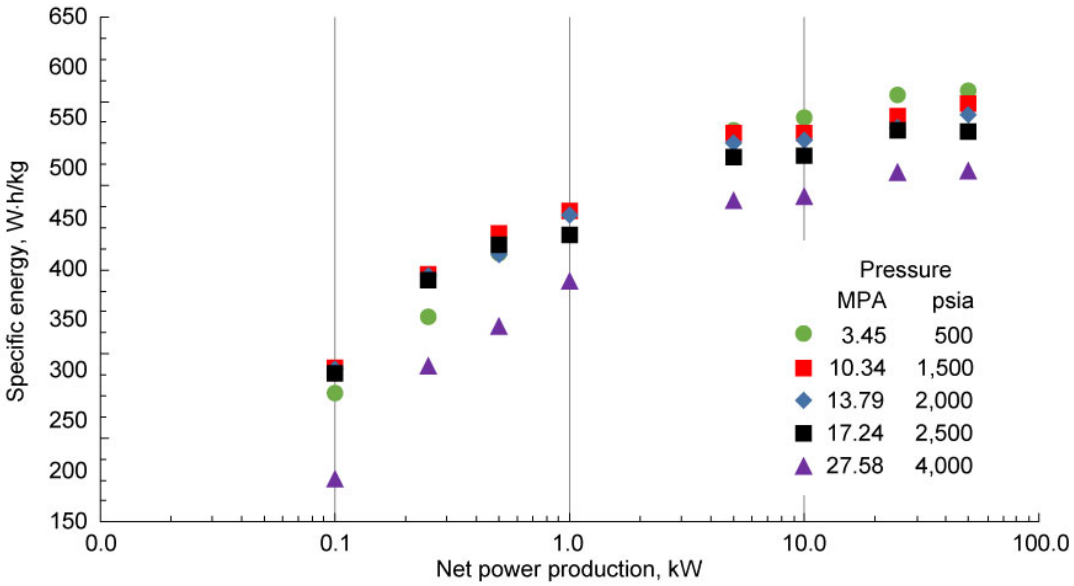

Figure 5.—Effect of electrolyzer operational pressure on regenerative fuel cell net specific energy at various power production levels.

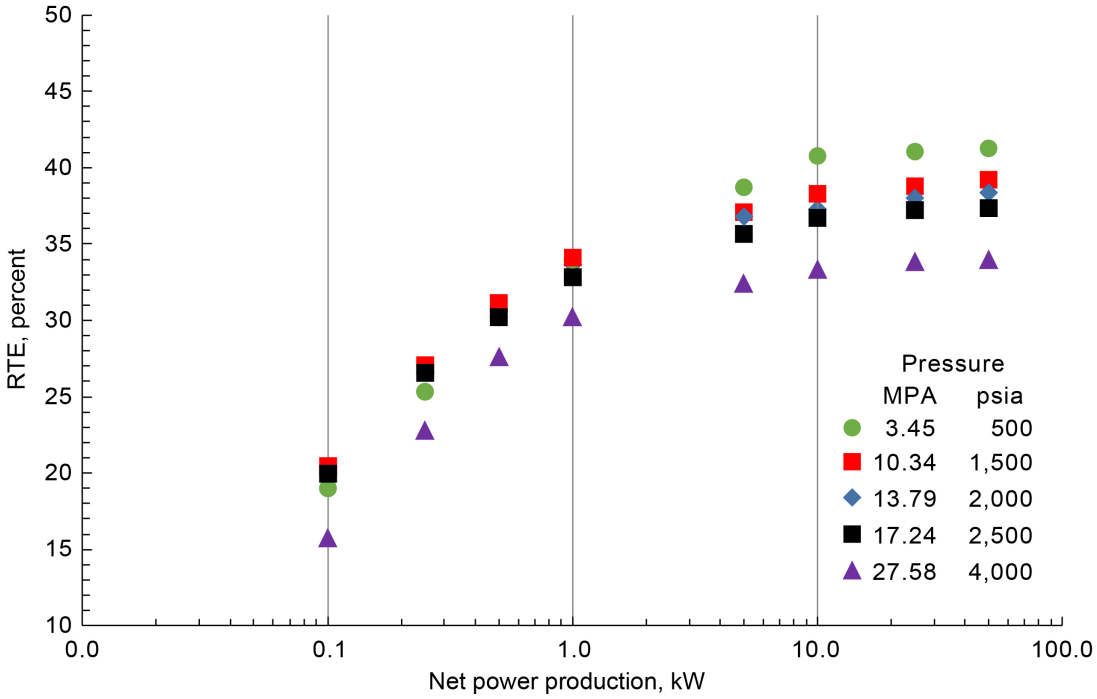

Figure 6.—Effect of electrolyzer operational pressure on regenerative fuel cell round-trip efficiency (RTE) at various power production levels.

The RTE results are similar to the specific energy results. Lowering operational pressure from 27.58 to 10.34 MPa (4,000 to 1,500 psia) improves efficiency in all cases, providing an increase of approximately 4 percentage points in RTE. Further reducing pressure from 10.34 to 3.45 MPa (1,500 to 500 psia) improves efficiency for RFCs of >1 kW, but that pressure change provides only equivalent or even slightly worse performance below that power level.

The RTE improvement as pressure decreases is mostly a result of reduced pressure-driven back diffusion losses in the EZ. In terms of current density, these diffusion losses equate to 25 mA/cm^2 at 3.45 MPa (500 psia) and 203 mA/cm^2 at 27.58 MPa (4,000 psia). Thus, in a load profile consisting of a design maximum current density of 1,000 mA/cm^2, 27.58 MPa (4,000 psia) operation automatically results in a greater than 20 percent efficiency reduction during all electrolysis periods. Without improved membrane technology, operation at such high pressures is impractical unless system volume is the primary performance metric: For a lunar equator RFC, reactant storage volume is ~95 percent of total system volume at any power level, and doubling reactant storage pressure effectively equates to halving the RFC volume.

3.3.2 Electrolyzer Power Profile

Solar power availability is not constant over a lunar day, as presented in Figure 7. Simply dividing a lunar cycle duration in half and assuming ~350 h for electrolysis may not be a satisfactory assumption. Thus, there is a question as to when and how electrolysis should proceed during this daytime period. For example, do customer load demands take precedence over energy storage? There is much uncertainty here depending on how integrated the energy storage system is with the lander or rover. Ideally, the customer loads, RFC system, and solar array should be designed together in order to maximize efficiency and solar energy utilization.

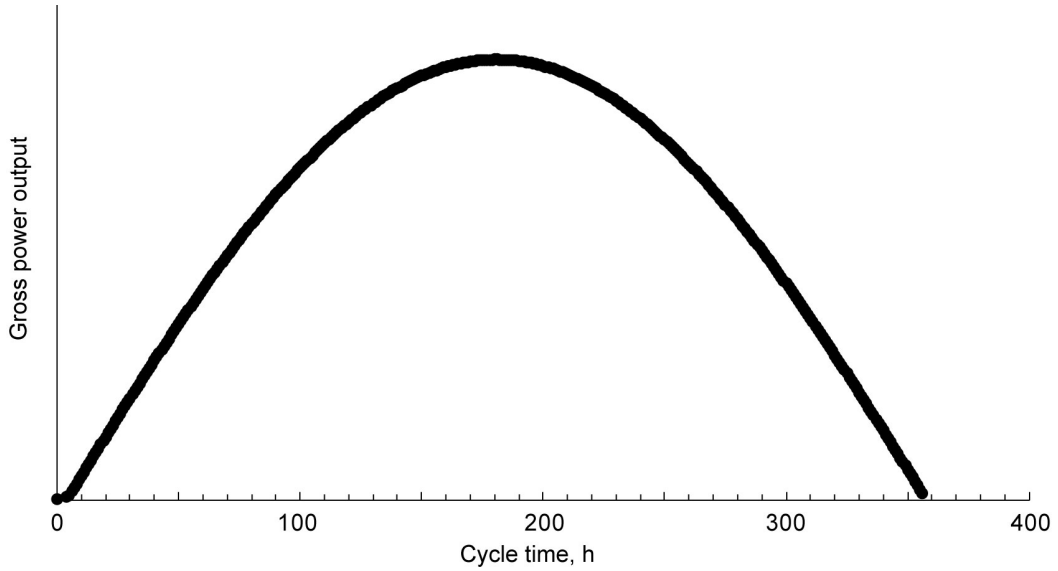

Figure 7.—Example solar array gross power output profile over lunar equatorial day. Cycle time 0 is time at start of solar power availability during cycle.

If a customer requires a constant 0.1 kW of electrical power during the daylight period, an EZ can be sized and the operation simulated to create load profile options. These load profiles are presented in Figure 8, Figure 9, and Figure 10 for 15-cell liquid anode feed EZs with active areas of 50, 100, and 150 cm^2, respectively, all operating at 10.34 MPa (1,500 psia). In each case, the stacks are generating the same total quantities of hydrogen and oxygen, and the daylight duration is a total of 357 h. Three stack sizes are included to evaluate the impact of a larger, higher-rate-capable EZ stack in the system design. Greater active area reduces the needed current density, thus reducing cell voltage and improving efficiency (Ref. 18). However, this improvement is counteracted by increased crossover losses.

The load profiles are modeled for a range of durations from the total daylight period down to the maximum rate capability of the EZ at a current density of 1,000 mA/cm^2. The slowest rate, or longest time, is noted with a multiplier of 1, where the RFC is sized for the minimum possible electrical input power that enables regeneration of the required hydrogen and oxygen quantities, and the profile matches that of the solar array profile in Figure 7. A multiplier of 1.25 means that electrolysis produces the product gases at a rate of 1.25 times that of the minimum rate case. The maximum rate and shortest electrolysis duration for a given stack size is represented by a constant load profile. Since the 50 cm^2 stack is minimally sized for a 0.1-kW-class RFC, it is not possible to increase the electrolysis rate as much as for the 100 and 150 cm^2 stacks.

The load profile significantly influences both EZ efficiency and RFC maximum input power, or charge power. Figure 11 displays that initially, increasing the electrolysis rate and reducing EZ operational time improves efficiency compared with the minimum rate case because back diffusion losses are pressure dependent rather than rate dependent. Increasing the current density results in a greater fraction of the input power going to producing product gases. At a certain point for each active area (<200 h for 50 cm^2, <100 h for 100 cm^2, and <75 h for 150 cm^2), mass transport losses begin to become significant, cell voltage increases, and EZ efficiency starts to diminish. For all three active area sizes modeled here, the peak EZ efficiency occurred for the load profile that represented the shortest duration, highest power profile that avoided any steady-state operation at constant power. Similar to these results, Ulleberg suggested that the EZ should operate in a variable power mode where the EZ only turns on when there is excess power and runs at a high current density, which enables more gas production and less interim battery usage (Ref. 8).

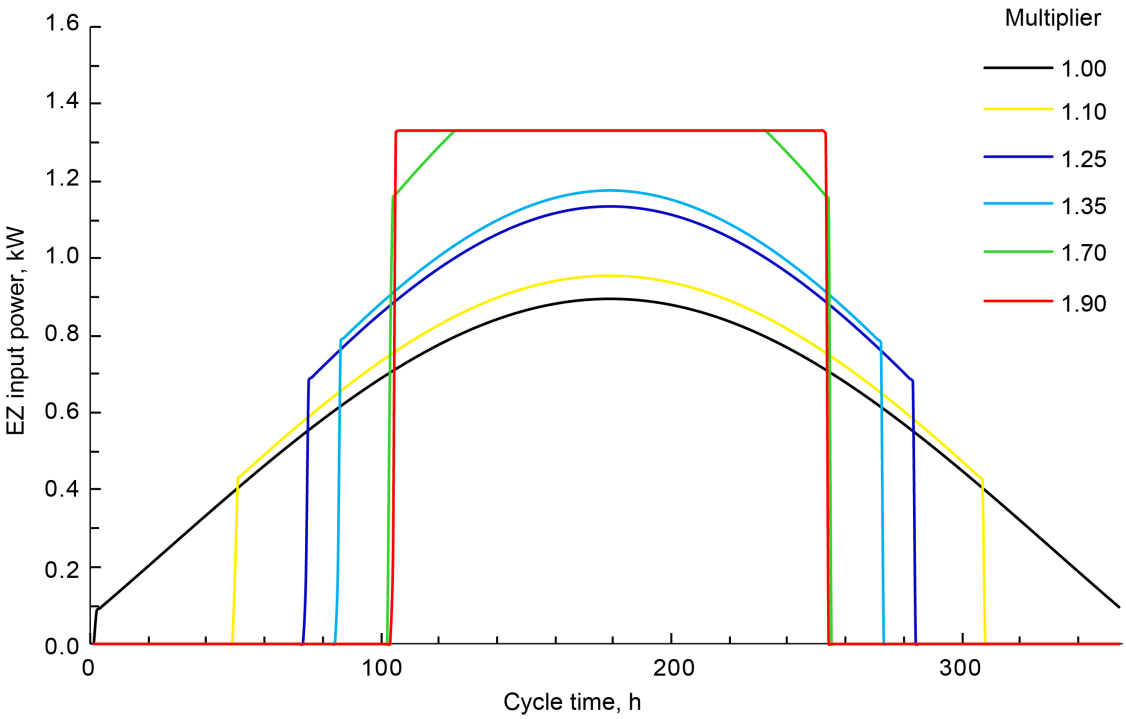

Figure 8.—Electrolyzer (EZ) input power load profiles for 15-cell stack with 50 cm^2 active area. Multiplier value used to calculate electrolysis rate compared with minimum rate case.

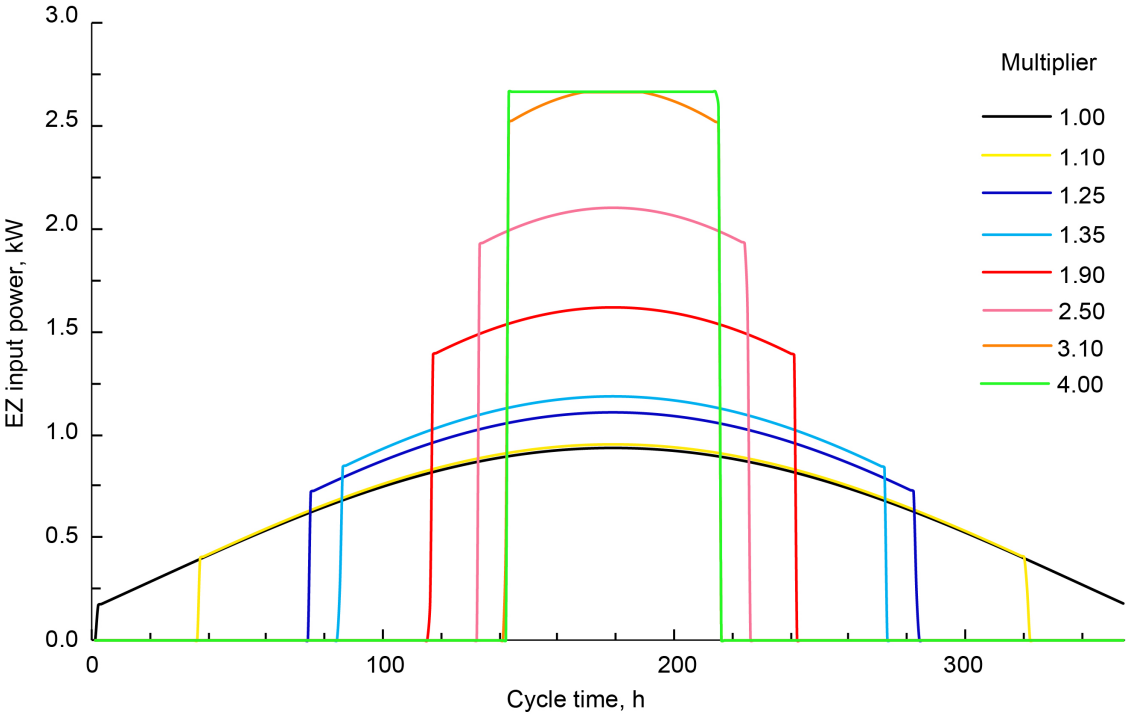

Figure 9.—Electrolyzer (EZ) input power load profiles for 15-cell stack with 100 cm^2 active area. Multiplier value used to calculate electrolysis rate compared with minimum rate case.

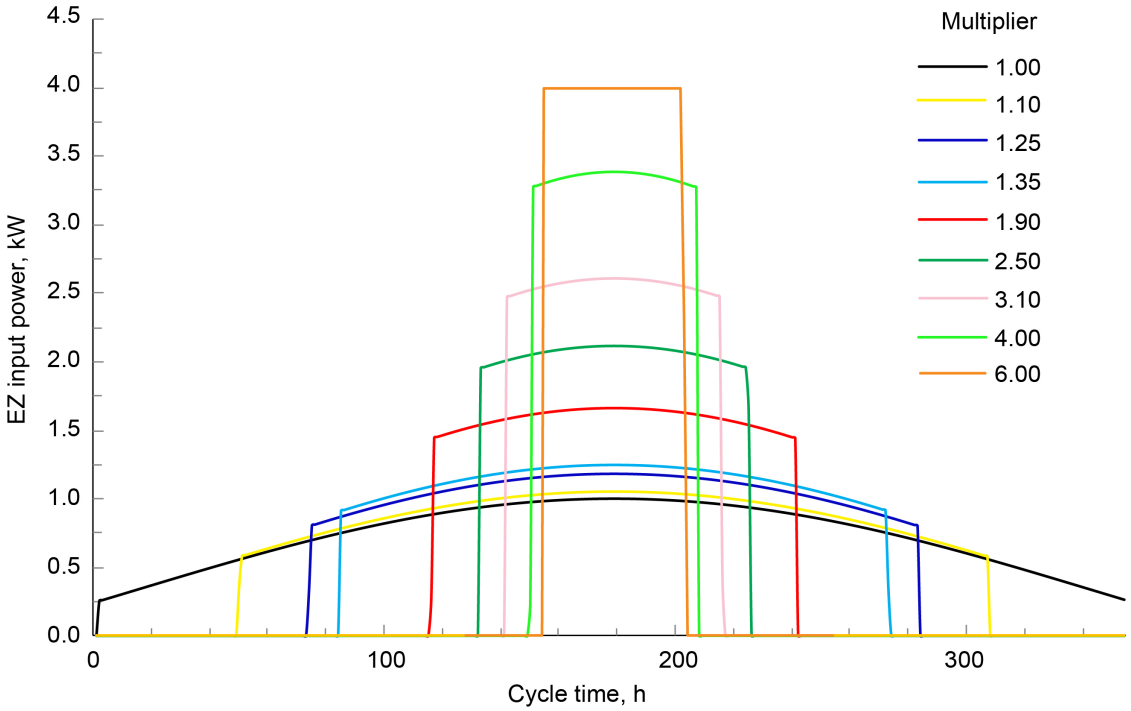

Figure 10.—Electrolyzer (EZ) input power load profiles for 15-cell stack with 150 cm^2 active area. Multiplier value used to calculate electrolysis rate compared with minimum rate case.

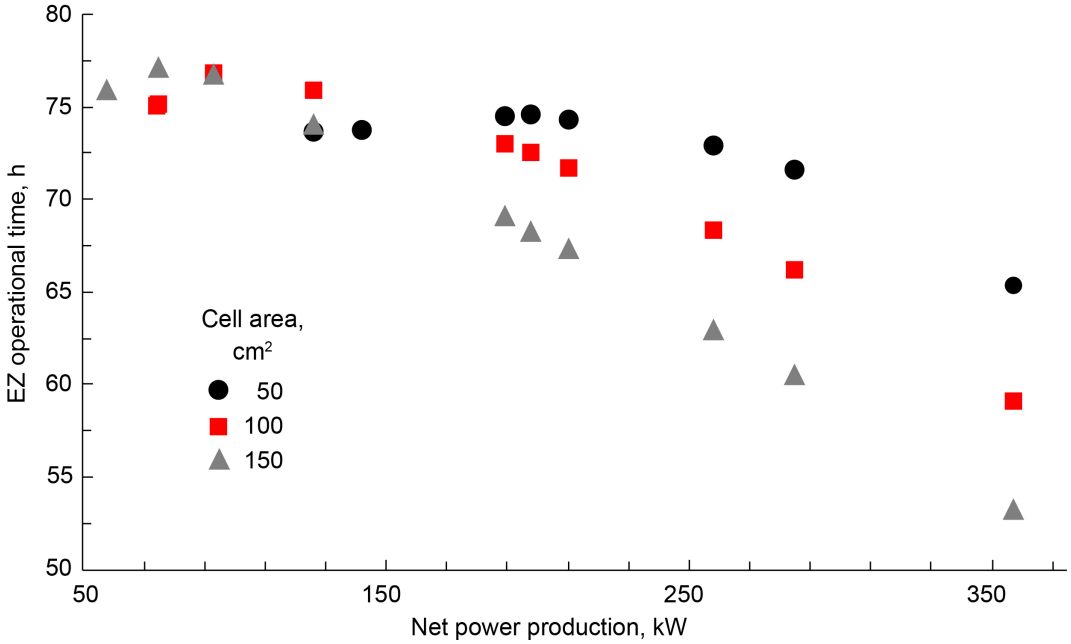

Figure 11.—Electrolyzer (EZ) overall efficiency at various electrolyzer operational times for 15-cell electrolyzers with either 50, 100, or 150 cm^2 active area per cell.

Actual EZ efficiency has been observed at 88 to 92 percent (Ref. 3). Much lower values are estimated here because of the higher operational pressure. Barbir noted that in high-pressure systems, it is preferable to operate at high performance levels (i.e., high current density) to minimize the consequences of crossover losses (Ref. 2). This can be accomplished by selecting a smaller EZ for use at a given recharge rate, but there are complex relationships with cell voltage performance and design operational pressure that must always be considered.

Highest efficiency does not necessarily equate to lowest mass and highest specific energy (Refs. 2, 6, and 21). Maximizing RTE can increase total stack masses by 2 to 5 times (Ref. 21), but stack mass is not the biggest factor for a lunar-equator RFC where reactant storage dominates total system mass and volume. Although highest efficiency and specific energy are generally in agreement throughout this publication, the two are not equivalent as design metrics, especially when considering the solar array power source in conjunction with the RFC. Solar array mass may make up ~70 percent of total system mass when considering an RFC plus PV array, so a designer must consider the complete system (Ref. 2).

PV power system mass decreases as RFC RTE increases (Refs. 2 and 4). Not accounting for any solar array degradation, an RFC with a 50-percent RTE requires a solar array capable of producing ~3 times the nominal RFC power, whereas it is ~2.5 times for an RTE of 60 percent and ~2.3 for an RTE of 70 percent (Ref. 4). Barbir estimated the total system mass to be 115 to 125 kg/kW at 25 percent RTE and 100 to 110 kg/kW at 30 to 35 percent RTE (Ref. 2). Improving RTE provides the opportunity to reduce solar array size, but improving EZ efficiency only partially counteracts the increased power required to operate an EZ at a higher rate. Figure 12 demonstrates that reducing the EZ operation time by two-thirds relative to the maximum 357 h minimally increases the maximum required solar array power for the stacks. Further shortening of the EZ operation time raises required solar array power so much that further efficiency benefits might not be worthwhile. The solar array power is the RFC charge power plus power to the customer. A system designer must balance the desire to improve efficiency with the charge power level. Requiring an oversized solar array could negate the efficiency improvement benefits.

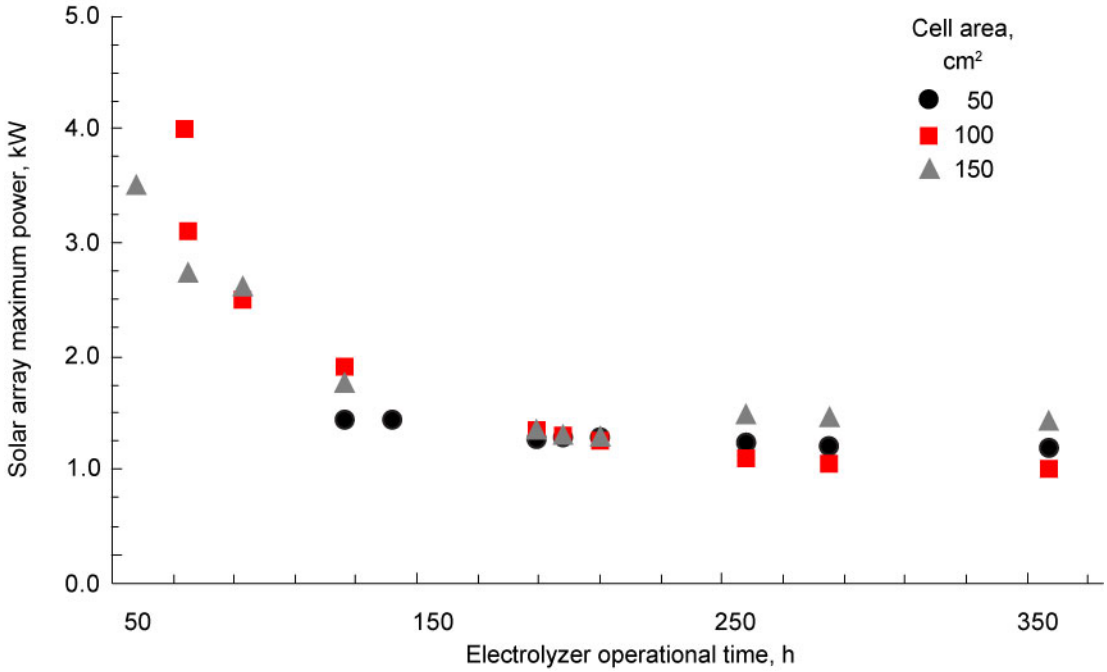

Figure 12.—Maximum power required from solar array to complete electrolysis cycle in various operational times for 15-cell electrolyzers with either 50, 100, or 150 cm^2 active area per cell.

3.3.3 Operational Temperatures

Figure 13 shows the effect of EZ average cell operating temperature on RTE. EZ operating temperature was set to 50, 60, 70, and 80 °C. Increasing temperature generally improves cell voltage performance, thus increasing efficiency (Ref. 18). There is a converse effect, however, in that membrane permeability also increases with temperature. At 10.34 MPa (1,500 psia) balanced pressure operation with a 0.25- mm- (0.010-in.-) thick membrane, there is gas crossover equivalent to 79 mA/cm^2 at 80 °C, but it is only 44 mA/cm^2 at 50 °C. This crossover impairs EZ efficiency enough to reduce RTE with increasing EZ temperature at any power level. Across the evaluated power levels, there is a 1 to 2 percentage point RTE decrease when raising temperature from 50 to 80 °C. Lower operating temperature is also known to reduce membrane degradation rates (Refs. 22 to 25), so lower operational temperature is clearly preferred if other compromises can be accepted.

The primary system-level reason to consider increasing EZ operating temperature is that radiator size reduces with higher EZ operating temperature. Levy noted that higher stack operational temperature improves stack voltage performance and eases radiative heat rejection (Ref. 26). For an RFC in a lunar environment where there are extreme temperature changes between day and night periods, the system radiator is most likely to be sized based on the daytime operation. Because it takes more power to charge an RFC than the FC produces (although EZs are more efficient than FCs) and the environmental temperatures are much cooler during FC operation (i.e., heat may be needed to maintain internal temperatures for RFC and the customer), an RFC must reject more heat during times when it also happens to be hottest. Therefore, a warmer EZ stack gives a greater temperature difference to the sink temperature, reducing the required radiator surface area. For example, for a 1-kW RFC system, a 3.9-m^2 radiator is needed at an EZ operating temperature of 50 °C, but that could reduce to 2.3 m^2 at 80 °C. If a lander design is particularly volume constrained, this may become a primary design factor. Unfortunately, there

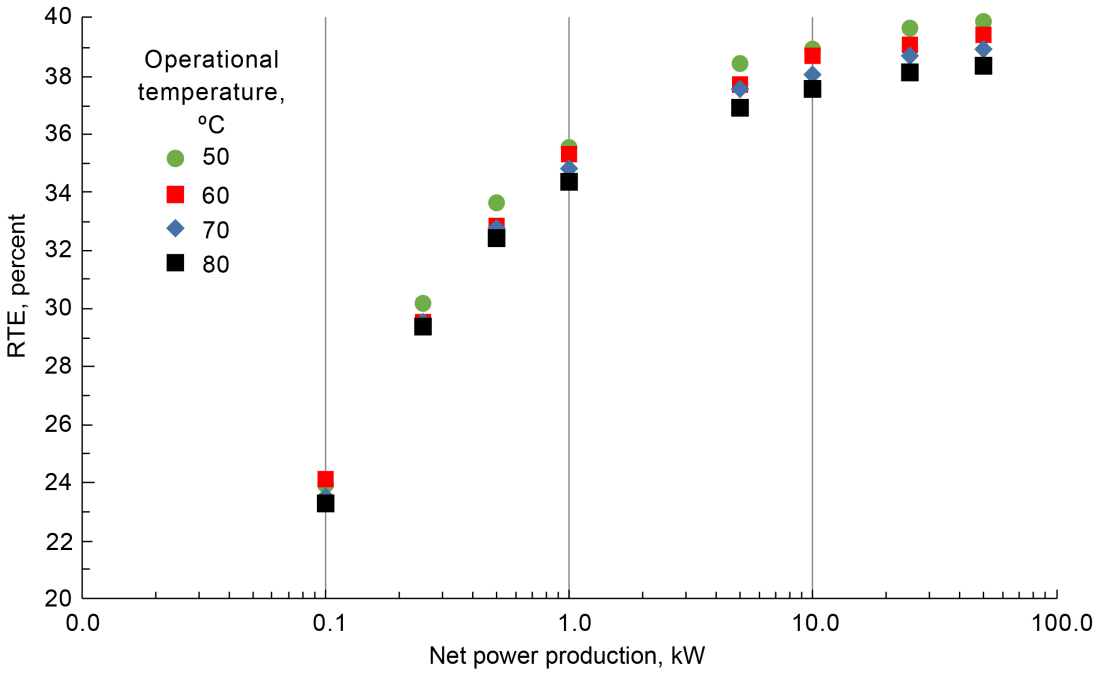

Figure 13.—Round-trip efficiency (RTE) over range of regenerative fuel cell power scales when varying electrolyzer average cell operational temperature and maintaining 10.34 MPa (1,500 psia) balanced pressure operation.

is a relatively narrow thermal operational range for PEMs, daytime lunar equator sink temperatures approach the typical operational temperatures, and increased gas crossover counteracts the cell voltage efficiency gains. In optimizing the system design, there must be a balancing of all these issues.

3.3.4 Electrolyzer Membrane Thickness

EZ efficiency and maximum solar array power were evaluated as a function of pressure for sulfonated-tetrafluoroethylene-based fluoropolymer-copolymer membrane thicknesses of 0.18 mm (0.007 in.), 0.25 mm (0.010 in.), and 0.51 mm (0.020 in.). Figure 14 shows that the 0.018-mm (0.007-in.) membrane enables the highest efficiency at 6.89 MPa (1,000 psia) or less, a 0.25-mm- (0.010-in.-) thick membrane provides the highest efficiency when operating at pressures between 6.895 and 17.24 MPa (1,000 and 2,500 psia), and the 0.51-mm (0.020-in.) membrane is best at above 17.24 MPa (2,500 psia). The relatively high ohmic resistance of the 0.51-mm (0.020-in.) membrane impairs performance versus thinner membranes at lower pressures. However, the thicker membranes do provide a benefit compared to the 0.18-mm (0.007-in.) membrane as crossover losses become more significant with increasing pressure. At 17.24 MPa (2,500 psia), the crossover current density is 127, 89, and 45 mA/cm^2 for 0.18-, 0.25-, and 0.51-mm (0.007-, 0.010-, and 0.020-in.) membranes, respectively.

There are alternative PEM materials that are known to reduce gas crossover, improve mechanical and thermal stability, and improve operational efficiency (Refs. 27 and 28). Accurate modeling requires real polarization curve data that were not available for the chosen stack technology in this analysis. In previous modeling efforts, 7-mil EZ membranes enabled EZ the efficiency to approach a maximum of 75 percent at 20.79 MPa (3,015 psia), 78 percent at 13.89 MPa (2,015 psia), and 89 percent at 1.48 MPa (215 psia) (Ref. 2). Accounting for parasitic loads, system efficiency during EZ operation dropped to 70 percent at 13.89 MPa (2,015 psia) (Ref. 2). The values reported from this work are lower, probably because of more conservative estimates of reactant crossover.

The solar array must produce the highest maximum power when paired with RFCs operating at either low (<6.89 MPa (1,000 psia)) or high (>24.13 MPa (3,500 psia)) pressures, as exhibited in Figure 15. The minimum for each respective membrane thickness occurs at higher pressures as membrane thickness increases. For example, the minimum for the 0.18-mm (0.007-in.) membrane occurs at 13.79 MPa (2,000 psia), whereas the minimum for the 0.51-mm (0.020-in.) membrane occurs at 20.68 MPa (3,000 psia). There is relatively little variation when the pressure is between 10.34 and 20.68 MPa

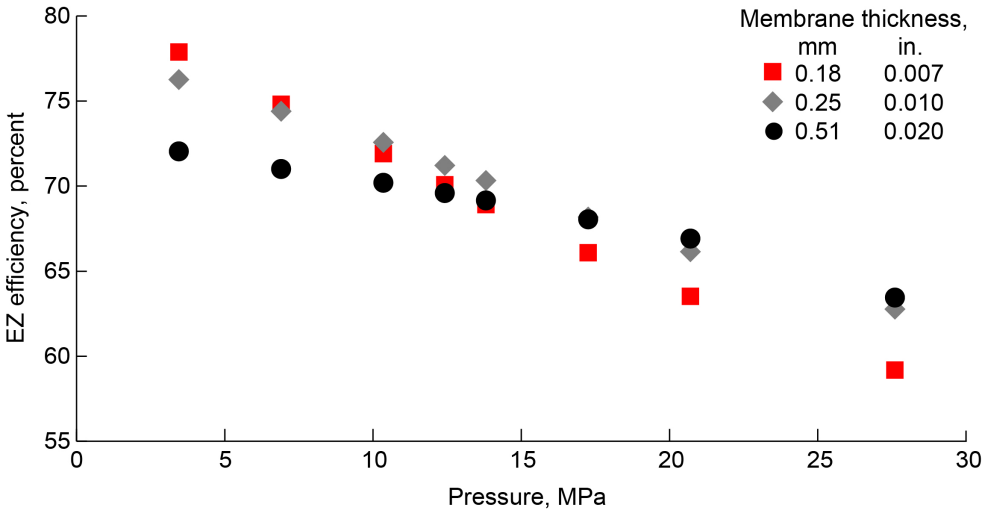

Figure 14.—Electrolyzer (EZ) efficiency over lunar equator cycle for range of operating pressures at different membrane thicknesses.

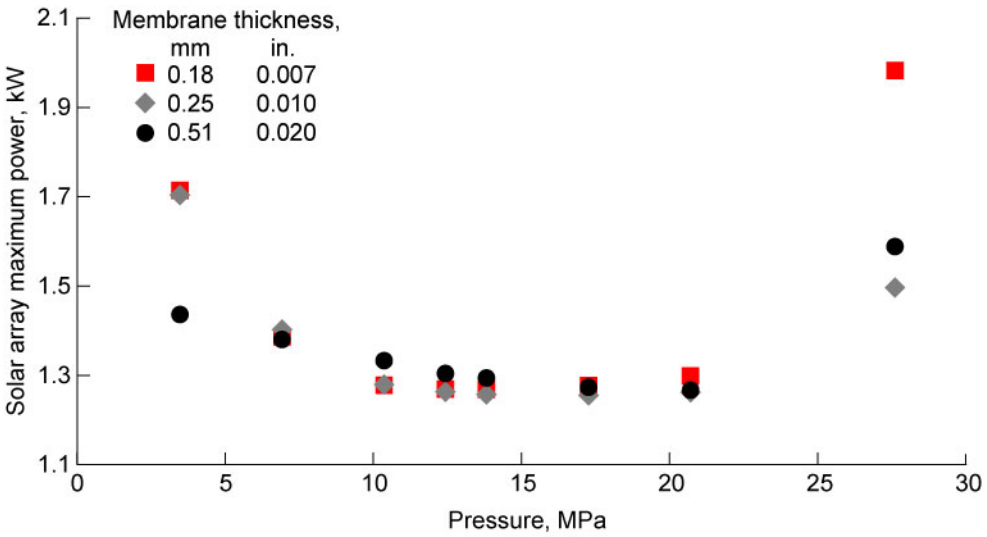

Figure 15.—Maximum regenerative fuel cell input power required from solar array for range of operating pressures at different membrane thicknesses.

(1,500 and 3,000 psia), but the minimum power required is achieved with 0.25-mm (0.010-in.) membranes at 17.24 MPa (2,500 psia). At high pressure, more solar array power for charging is required to compensate for the reduced EZ coulombic efficiency. At low pressure, reactant storage vessels become much larger and need more heat to remain in the acceptable thermal range. This is power that must be generated by the FC, so more reactant generation is needed during the EZ charge cycle, increasing the maximum needed input power.

3.4 Fuel Cell Stack Sizing

FCs generally become more efficient if sized larger in order to operate at lower current densities and higher cell voltages (Refs. 2 and 8). Therefore, it has been suggested that FCs should be oversized to allow for relatively low power operation (compared to the maximum power generation capability of a stack) and be on as much as possible, while still avoiding operational modes that reduce operating life such as frequent starts and stops or staying at high open-circuit cell voltages (Ref. 8). The long cycle durations and infrequent switching at the lunar equator along with appropriate mission design to avoid frequent shading make the start-stop constraint unlikely to be a problem. More switching is likely at the lunar south pole or other shorter duration cycle locations, in which case additional constraints may be needed, such as minimum run times (used for terrestrial stationary systems supporting solar arrays).

There are existing evaluations of individual stack-level performance issues on PEM FCs of the type modeled here (Refs. 29 and 30). Unfortunately, just like with EZs, many parameters that improve cell voltage performance (reduced membrane thickness and increased pressure or temperature) also increase reactant crossover rate, which counteracts the overall efficiency improvement. Crossover would also increase with active area. To evaluate the effect of FC sizing as a function of nominal operational current density on RFC RTE, Figure 16 shows the resulting RTEs for three different RFC scales at five different current densities. At each power level, stack active area was adjusted in response to the input current density, keeping RFC net power output constant. For 0.1-, 1-, and 10-kW RFCs, operating near 100 mA/cm^2 provided the highest RTEs. Above this current density, cell voltage decreases reduce RTE. Below 100 mA/cm^2, the constant crossover becomes more impactful compared to the reduced current density setpoint. It has been noted that oversizing stacks makes any standby low-power-mode operation

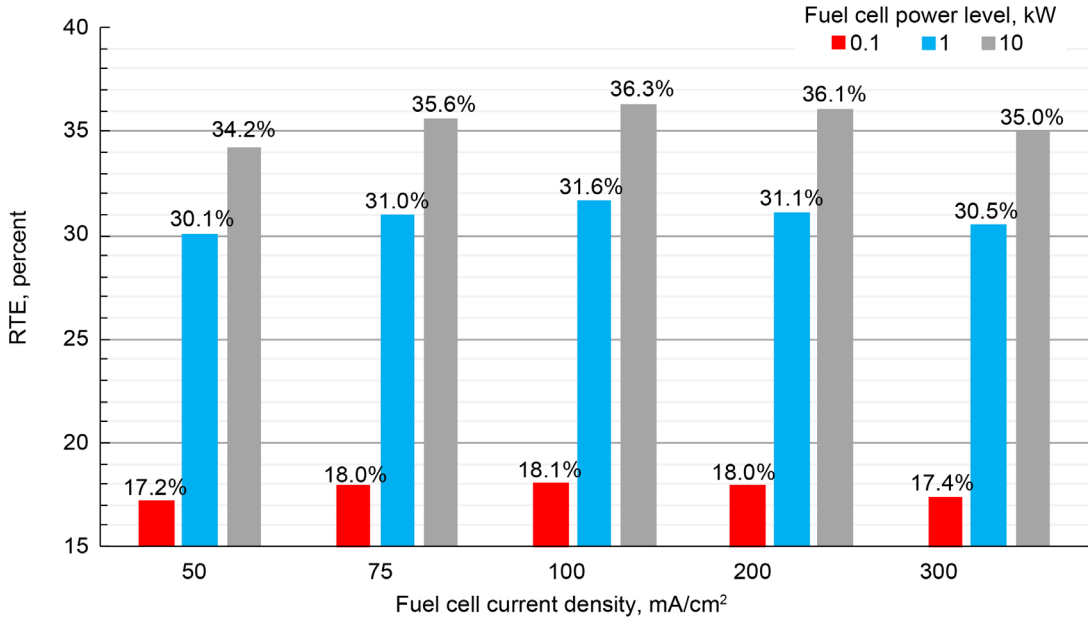

Figure 16.—Round-trip efficiency (RTE) as function of fuel cell design current density for three different regenerative fuel cell scales.

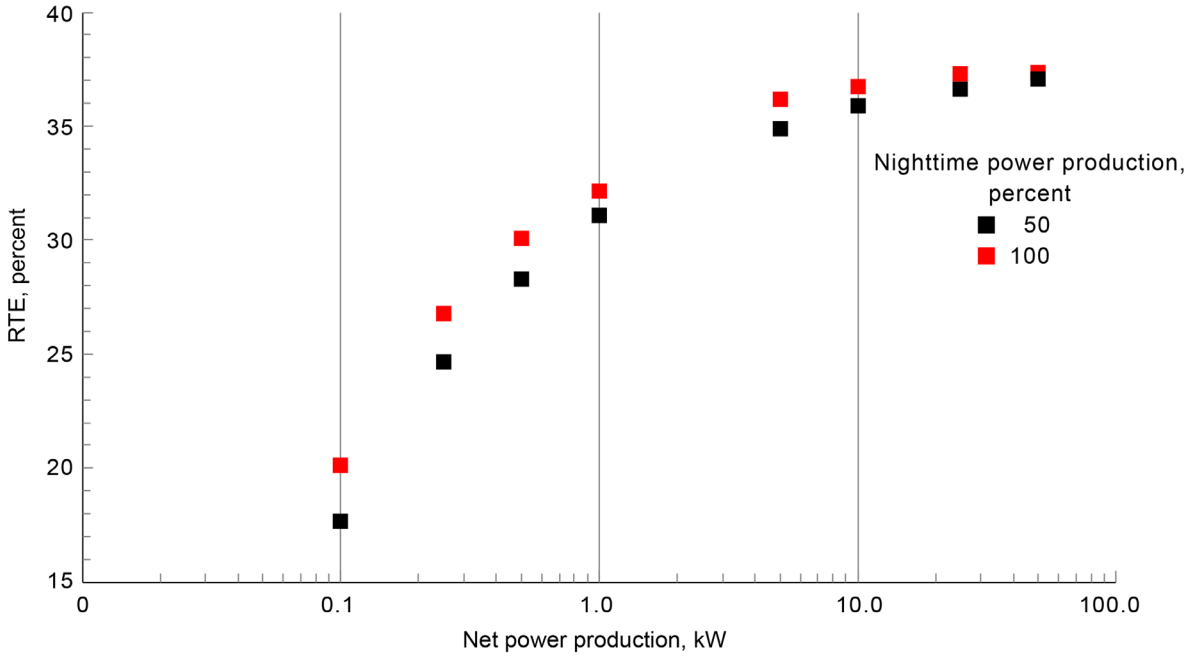

Figure 17.—Round-trip efficiency (RTE) at various regenerative fuel cell scales for systems that produce 100 percent of rated net power compared to systems that produce only 50 percent of rated power during lunar nights.

very harmful to RTE (Ref. 18). If long-duration standby modes are a significant part of a mission profile, the published advice to pursue low FC current densities may be counterproductive. Different assumptions on cell voltage as a function of current density, load profile, and rate of crossover will alter the optimal point for every FC so there is no ideal compromise for all systems.

In the majority of this report, it is assumed there is no reduction in customer power demand during lunar night intervals. Unmanned missions such as in situ resource utilization schemes may have reduced

power loads during periods of eclipse. Figure 17 displays the resulting RTEs when nighttime net power demand is reduced to 50 percent. For any given RFC scale, lower RTEs resulted from the reduced nighttime power demand case. This is a function of sizing RFC components to produce a nominal power level, but not operating there for a large fraction of the time. Any FC will be most efficient if operating at a constant rate, matching the designed peak efficiency point. Realistically, reducing nighttime power requirements is an effort to minimize total system mass, volume, and the daytime charge power needs and still provide enough power to allow the customer to survive lunar night conditions.

3.5 Component Considerations

3.5.1 Stack Bus Versus Voltage Converters

Although utilizing voltage converters eases system engineering by establishing a more definable interface, there is an efficiency penalty and the converters likely require cooling. As noted in the section on parasitic load rankings (see Sec. 3.2), voltage conversion losses are the primary parasitic drag during RFC charging and are only behind storage vessel heating and solenoid valve power consumption during RFC discharging for a 0.1-kW RFC. As the RFC scale increases to higher power levels, valve power becomes less impactful, but the voltage regulation losses will always remain the same approximate fraction. Therefore, these are clearly an important design consideration.

A more efficient method of powering the EZ is to connect directly to an optimally sized solar array so that voltage floats with the array output, replacing the voltage converters with a simple high-current relay. Such a switch would be more efficient than the converters, increasing the RTE 3 to 5 percentage points. However, this modification would limit the ability to control the current into the EZ other than connecting or disconnecting. Communication with or control over the solar array output could mediate this. Even though this concept could be incorporated into an RFC, it is likely not applicable for missions where the RFC would be considered a payload. The design requires significant system-level planning and integration. This has implications regarding scalability and portability of the resulting design.

Figure 18 presents a comparison of RFC RTE for 100 percent voltage regulation efficiency (direct connection of input and output power to electrochemical stacks) compared to 95 and 90 percent conversion efficiency on both the electrical input and output, respectively, which is approximately what could be expected from existing converters. Chang assumed 95 percent voltage converter efficiency and only 2.3 kg/kW for PMAD mass whereas this model assumes 10 kg/kW, based on Reference 31. Along with reactant storage pressure, this is one of the most impactful design considerations in attempting to improve RTE.

3.5.2 Solenoid Valve Options

In the RFC system, the reactant gases are stored at high pressure, the FC operates at low pressure, the product water is stored at low pressure, and the EZ operates at high pressure. With multiple fluids present, as many as 15 individual solenoid valves could be required to isolate the high pressure differentials.

For a 0.1-kW-class RFC, the parasitic power consumption from solenoid valves is significant (see Sec. 3.2). Though not all valves are powered simultaneously, operating five 10-W valves is considerably detrimental to the overall efficiency when delivering only 0.1 kW net power. As presented in Figure 19, there is a general relationship between valve differential pressure management capability and power consumption. A survey of commercially available valves shows that relatively few valves are available for high pressures and none at low power levels, typically less than 2 W, thus requiring the use of a higher power valve.

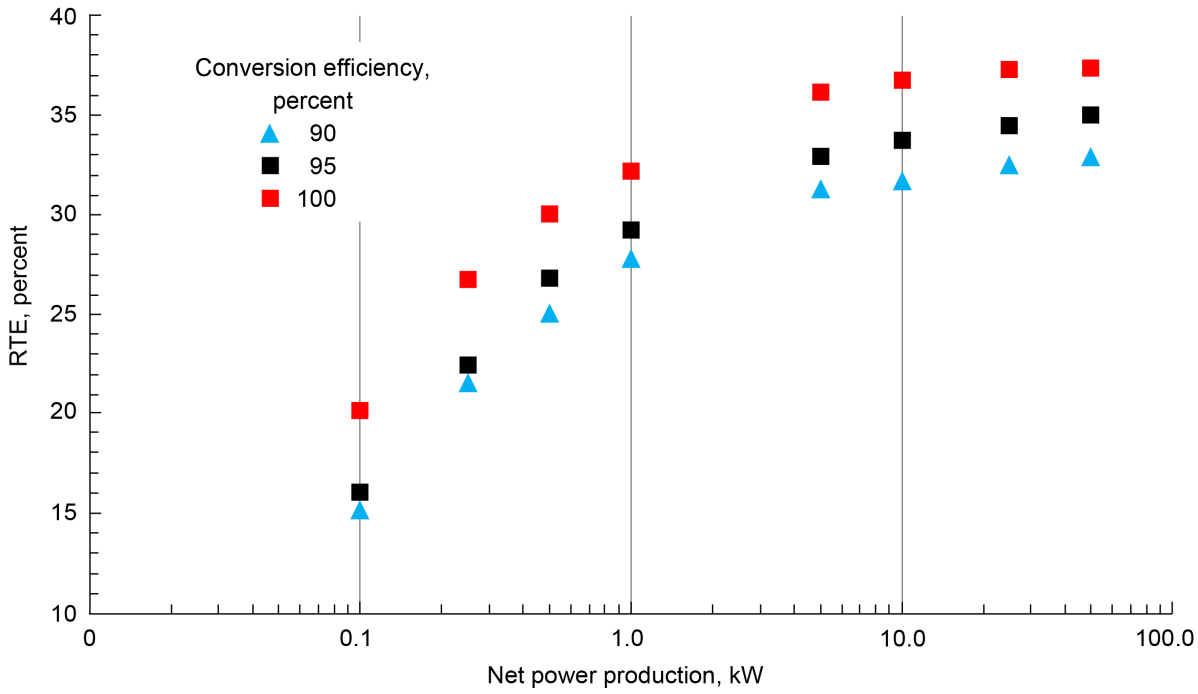

Figure 18.—Regenerative fuel cell (RFC) round-trip efficiency (RTE) over range of RFC scales including 90, 95, and 100 percent voltage conversion efficiency for input and output power.

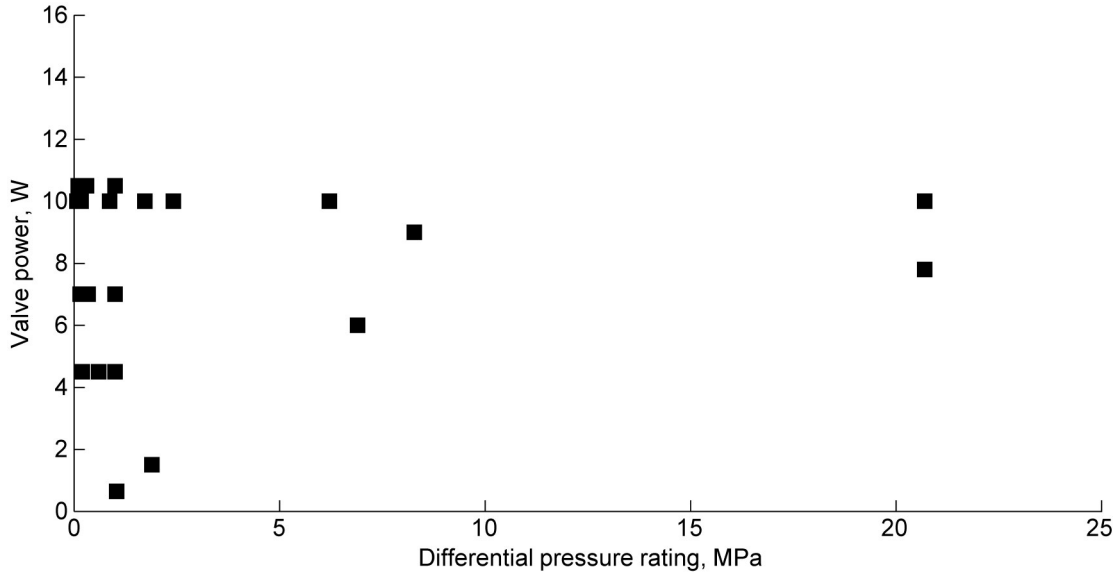

Figure 19.—Relationship of solenoid valve power consumption to differential pressure rating.

One option for reducing this load is to utilize latching solenoid valves. These solenoids require bidirectional power but only during state changes. There is no steady-state power consumption. There are two primary disadvantages to these devices. One is that the solenoid coils tend to be weaker than standard solenoids and have more limited operational ranges as a result. For example, when a valve is designed to operate at certain nominal supply and outlet pressures, it may fail to respond when off-nominal pressures provide additional resistance to valve movement. A few vendors offer latching products without this constraint, but the cost is relatively high, approximately $50K per unit. Second, latching valves present

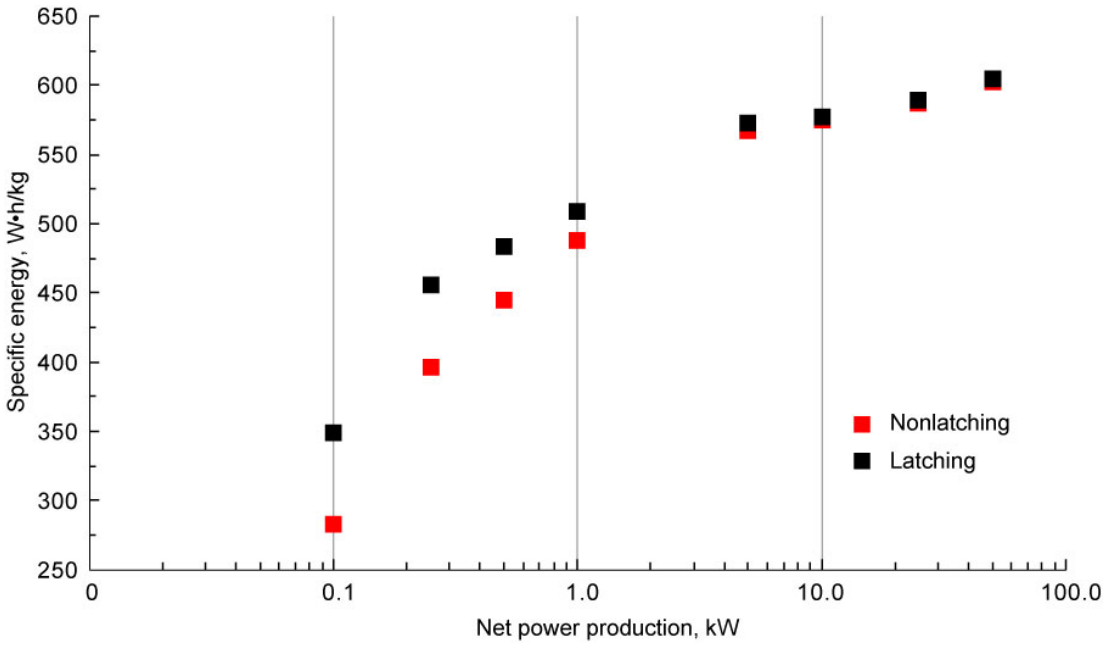

Figure 20.—Specific energy comparison for regenerative fuel cell systems with and without latching solenoid valves.

safety concerns in manned or safety-critical applications. In the absence of power, the valves do not necessarily default to a fail-closed or fail-open state. This may result in loss of command, inadequate safe-stating, or uncertainty regarding system status in the event of a failure.

For a range of RFC net power outputs from 0.1 to 50 kW, the resulting specific energy was determined for systems with and without latching solenoid valves. These results are shown in Figure 20. Specific energy is always higher for systems incorporating latching valves, but the difference is negligible beyond the 1-kW class. The number of solenoid valves does not scale with RFC net power output, so although larger solenoids consume more power, there is little benefit to using latching valves when the net power output is 2 orders of magnitude greater than the parasitic load. For smaller RFCs, however, specific energy may be improved by more than 20 percent simply by selecting latching solenoids.

Another alternative to mitigate the standard solenoid parasitic load is by operating valves in a spike-and-hold manner. This involves initially powering valves at the rated operational voltage, waiting for an open or close response, then reducing the voltage to some lower value that still maintains the desired valve position. Initial testing shows that this practice is more repeatable and effective for higher power valves, meaning a nominal 10-W valve may remain open at 1 W, whereas a nominal 2-W valve may also require 1 W or even more to remain in the desired position. Given that miniature 2-W valves have provided inconsistent performance in previous FC systems, there seems to be little real advantage in the application of nominally low power valves. In absolute and percentage terms, spike-and-hold operation provides more benefit for valves rated to operate at higher power consumption levels.

3.6 Reactant Storage Considerations

3.6.1 Reactant Storage State

In the best-case scenario for the baseline 0.1-kW RFC at the lunar equator, a liquid anode feed EZ charging at a constant 1.07 kW can be expected to consume 173 g H_2O per hour. This produces 154 g O_2 per hour and 19 g H_2 per hour. Assuming an EZ operating at 0.70 MPa (102 psia) balanced pressure, 333 K, 90 percent electrical efficiency, a ratio for electrical energy input to thermal energy removed of

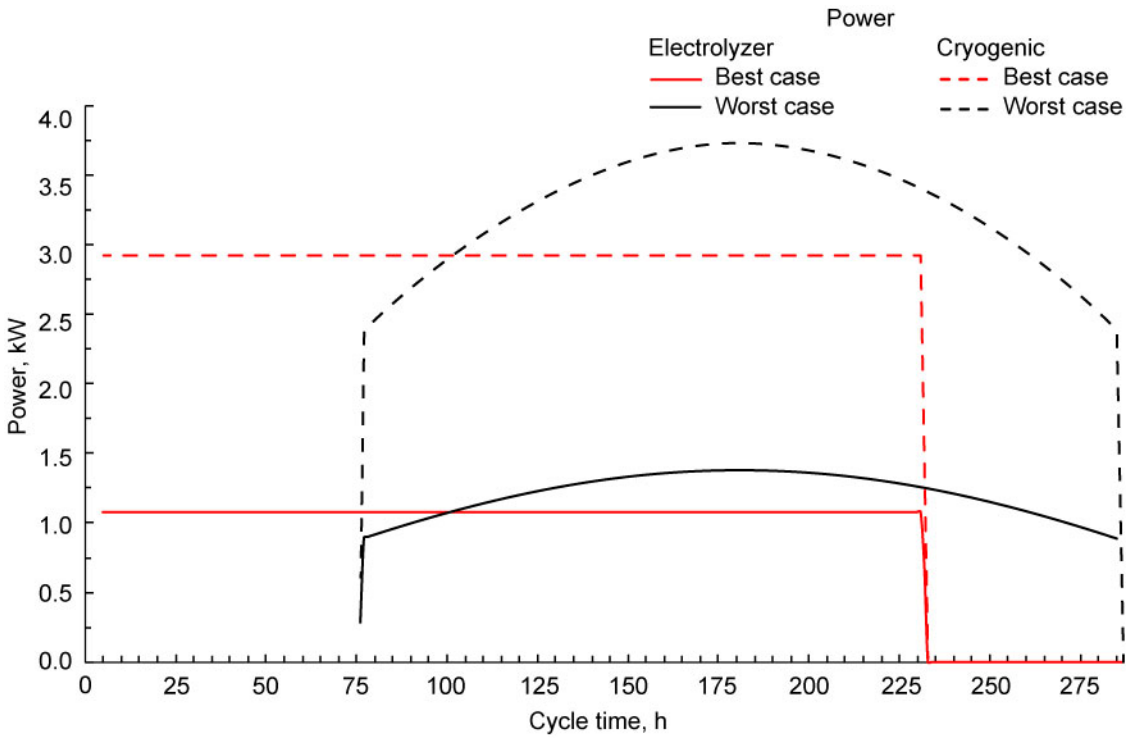

Figure 21.—Comparing electrolyzer stack power input and liquefaction power required to cryogenically store hydrogen and oxygen as generated during best- and worst-case daytime lunar equator cycles.

15:1 for O_2 and 80:1 for H_2, and a 30-percent volume margin on spherical tanks, the electrical power required to liquefy and maintain H_2 and O_2 during electrolysis can be calculated. For the best case, a constant 330 W are required to liquefy O_2 and 2,600 W are required to liquefy H_2. Because of the variable EZ load profile in the worst case condensed over a shorter part of a lunar day, the peak cryogenic power loads are higher: 430 W to liquefy O_2 and 3,300 W to liquefy H_2.

Figure 21 shows the EZ load profiles and cryogenic power loads for the best- and worst-case cycles. Electrolysis does not begin at the same time in each case since adequate solar power is available sooner in a cycle for the best case compared to the worst case. The cryogenic power loads are ~3 times the electrical power input required for the electrolysis and all other balance-of-plant (BoP) loads combined. This makes it impractical to integrate cryogenic storage into an RFC system. Any reactant storage volume or mass reduction benefit is more than negated by the reduction in efficiency and increase in required solar array size.

The RTEs for RFCs utilizing cryogenic storage are compared to gas storage at 10.34 MPa (1,500 psia) in cylindrical vessels in Figure 22. Rather than achievable RTEs exceeding 40 percent, no modeled cryogenic case could produce an RTE exceeding 15 percent. Cryogenic storage does eliminate the need for tank heating, but that parasitic power load is negligible compared to that of liquefaction. In addition, power would be required to maintain the liquefied state and to gasify the reactants for FC use, so the RTEs in Figure 22 are an upper bound for cryogenic storage. Cryogenic storage is ideal for permanently shadowed locations (Ref. 9), and lunar locations with large temperature swings do not provide that environment.

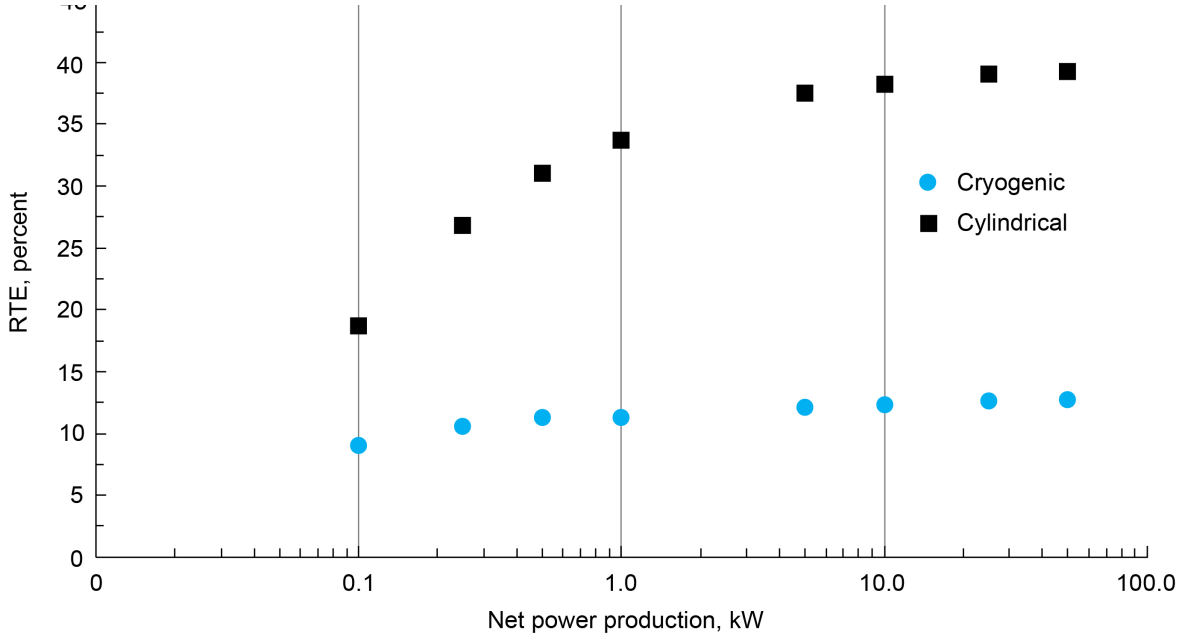

Figure 22.—Round-trip efficiency (RTE) for regenerative fuel cells utilizing either 10.34 MPa (1,500 psia) gas storage in cylindrical vessels or cryogenic storage in spherical vessels.

3.6.2 Gas Storage Vessel Configuration

The chosen reactant storage method is impactful for RFC system metrics. For all but the smallest systems, which may reasonably be replaced by batteries anyway, the reactant and associated storage vessels constitute the majority of the total system mass and volume. In addition to reactant storage pressure, the selection of vessel form factor is important. Theoretically, spherical vessels provide the lowest mass- and surface-area-to-volume ratio. Surface area is important in determining thermal requirements related to the reactant storage; however, there are very few, if any, commercially available spherical composite pressure vessels for hydrogen and oxygen storage. All steel vessels of any shape are prohibitively massive for flight applications. It is worthwhile to know if immediate development of scalable spherical pressure vessels would benefit RFC applications.

Figure 23 presents the impact storage vessel shape has on RTE across a range of RFC scales. The difference between the vessels is primarily the improved volume-to-surface-area ratio of spherical vessels compared to cylindrical vessels, which reduces the thermal energy required to heat the vessels during the lunar night. Chang reported that spherical storage vessels required 17 percent less heating power for their RFC system (Ref. 4). However, as RFC net power production increases, the benefit of spherical storage vessels decreases because of the decreased effect of heater power on the total parasitic load (see Sec. 3.2.1). Although heater power is the most significant parasitic load for the smallest RFCs, it becomes a less significant issue for larger systems. At 50 kW net power output, storage vessel heating power is equivalent to only 2 to 5 percent of the net power rather than ~80 percent for a 0.1-kW RFC.

Still, spherical vessels are advantageous when compared to cylindrical vessels because of the mass benefit. RFCs with spherical vessels have total system masses that are only ~2/3 that of RFCs with cylindrical vessels. Thus, vessel shape has a much greater impact on system specific energy. Figure 24 shows specific energy for spherical and cylindrical vessels in RFCs from 0.1 to 50 kW. There is an ~50 percent benefit for spherical vessels across the entire range.

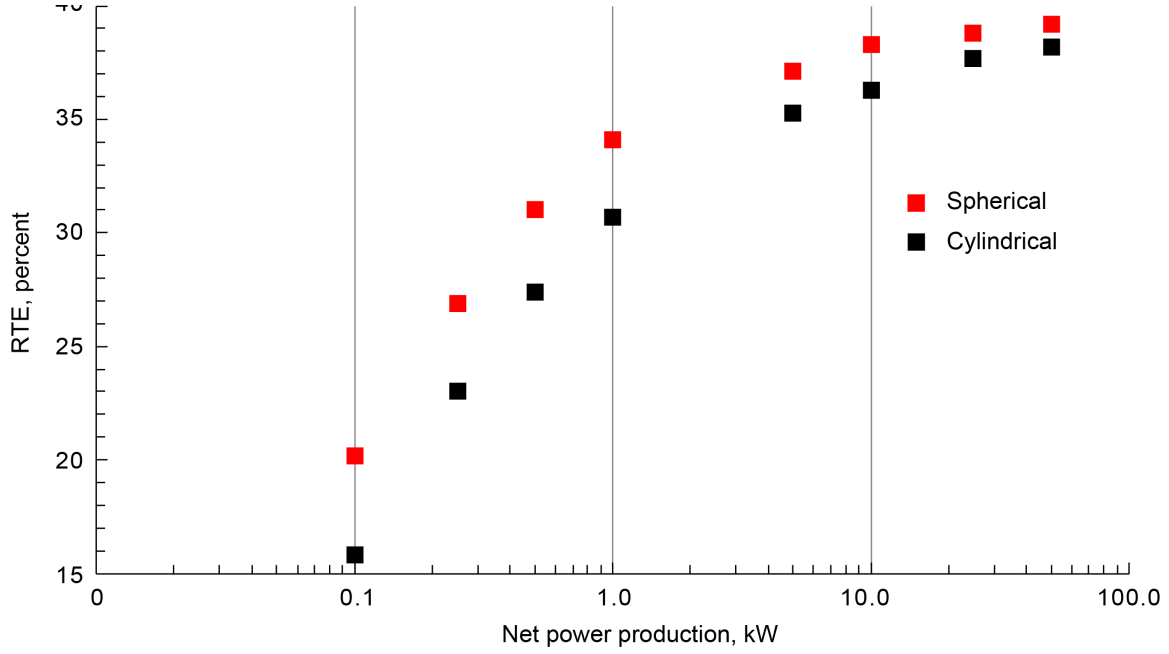

Figure 23.—Regenerative fuel cell round-trip efficiency (RTE) at various net constant power production levels when using either single spherical or cylindrical reactant storage vessels for hydrogen and oxygen gases.

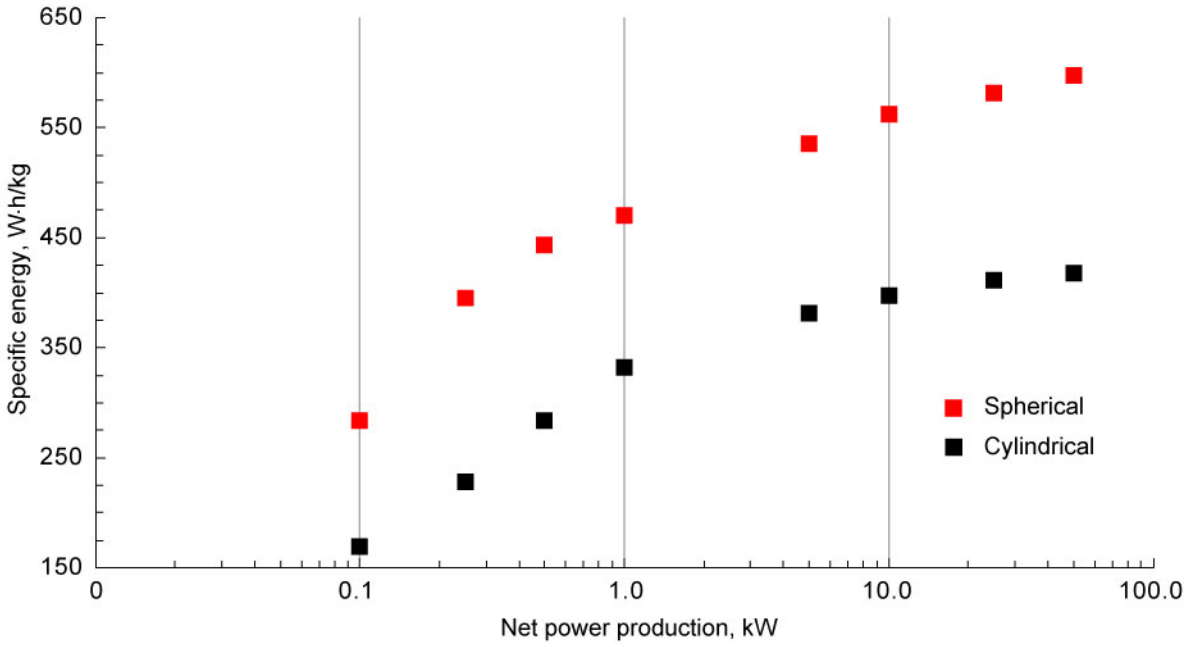

Figure 24.—Regenerative fuel cell net specific energy at various net constant power production levels when using either single spherical or cylindrical reactant storage vessels for hydrogen and oxygen gases.

3.6.3 Reactant Storage Temperature

As previously discussed (see Sec. 3.2.1), reactant storage vessel heating power is potentially the most significant parasitic load during FC operation. Although reactant storage vessels are not contained within the primary RFC thermal enclosure, the tanks must still be thermally regulated for multiple reasons. At the low lunar night temperatures, liquefaction of oxygen and formation of ice are likely. If the oxygen reactant becomes a liquid, the FC might be deprived of an adequate oxygen gas supply. The exact transition temperature depends on the RFC state of charge, or quantity of oxygen in the tanks. For a reactant tank initially charged at 10.34 MPa (1,500 psia) and 60 °C, the transition from gas to vapor to completely liquid occurs as the temperature drops from –100 to –173 °C. At an assumed minimum fill level of 20 percent of initial charge (the condition at the end of FC operation during the lunar night cycle), the vessels must be kept above –120 °C to maintain a supply pressure greater than 0.70 MPa (100 psia). Below this inlet pressure, gas regulator operation could be noticeably affected. Since the critical point of oxygen is –118 °C and 5.00 MPa (725 psia), operation throughout these temperature and pressure regimes can greatly affect the oxygen storage pressure.

If water left over from electrolysis forms ice within narrow flow passages found throughout an RFC, even a larger scale one, this ice can block either reactant from reaching the FC stack. This would effectively render the RFC useless and has long been a design challenge for RFCs utilizing water. One NASA demonstration used separation schemes to remove water, but they could not completely eliminate water from reaching the gas storage vessels (Ref. 18). Water in EZ product gases also must not be lost because that reduces RFC energy storage capacity (Ref. 4). For the case where water cannot be completely removed from the product gases, the storage vessels must be kept above the freezing point of water. When designing a short-duration, high-power, frequent-cycling RFC with reactant storage vessels inside the same thermal boundary as the electrochemical stacks, Chang made a similar assumption that heating would be required throughout the RFC to maintain all sections above the dew point temperature (Ref. 4). This was done in part because the authors noted that some heating would always be necessary and additional heating resulted in a simpler overall system compared with adding multiple separator units.

In Figure 25, the required heating power to maintain the vessels above various set temperatures during the lunar equator night for the baseline 100-W nominal RFC case is estimated. When no heat is provided, all vessels reach a –197 °C minimum temperature. This temperature is unacceptable not only because of media phase change concerns, but also because of tank material compatibility with such cold temperatures. For the lunar equator, a >0 °C thermal requirement results in 83 W of heat needed in a system producing only 100 W net power out (see Sec. 3.2.1).

The intermediate cases demonstrate how much parasitic power can be reduced through relaxed tank heating needs. Only 38 W are needed to maintain the vessels above –50 °C, which is still a realistic operational temperature for many commercially available composite pressure vessels. The impact of percentage point improvements in RTE was discussed in an earlier section (see Sec. 3.1). Changing the heater setpoint from 4 to –50 °C improves RTE by over 19 percent and reduces total system mass by 16 percent.

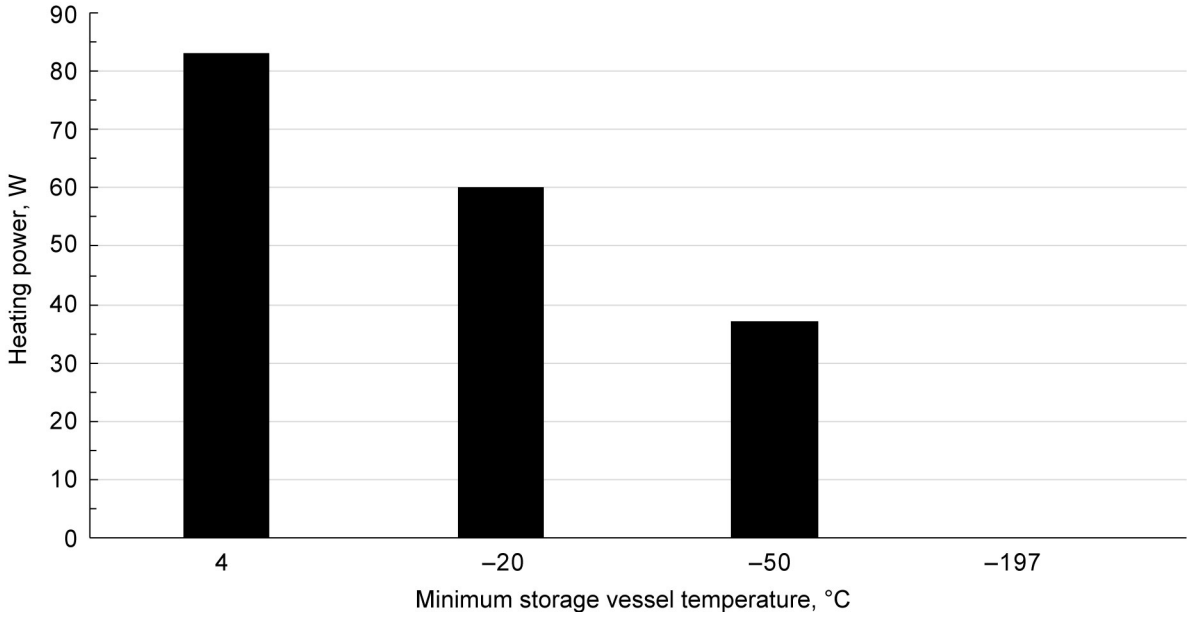

Figure 25.—Heating power required to maintain cylindrical storage vessels above set temperature for baseline 100-W regenerative fuel cell case. The –197 °C temperature represents resulting condition when no heat is applied.

4.0 Comparison to Previous NASA RFC Studies and Implications for Future Missions

NASA has long aimed for an RFC RTE goal of 55 percent (Ref. 26), which still aligns with current targets, but the specific energy goal has advanced considerably (from 110 to 550 W·h/kg). This modeling shows that the specific energy target is achievable at larger scales, but the RTE goal is a challenge for a lunar equator location. Although it is possible to approach 50 percent RTE in demonstration when considering only stack efficiencies, accounting for parasitic losses seems likely to drop efficiency into the 30 to 40 percent range. Improving practical RTE values requires further development of BoP components and high, balanced pressure EZ performance.

Table IV presents other reported RFC specific mass and RTE metrics, resulting from either modeling or demonstration, arranged by date and for multiple electrochemical technologies. None of the cases outlined in Table IV are based on lunar equator conditions, and all anticipated much shorter cycle durations in comparison. These and other variations in assumptions make comparing with results in this report difficult, though Titterington in 1970 estimated an RTE maximum of 41.5 percent at 3.45 MPa (500 psia) and 37 percent at 6.89 MPa (1,000 psia) (Ref. 18), which compares well with the 41.3 percent at 3.45 MPa (500 psia) and 38.1 percent at 10.34 MPa (1,500 psia) calculated in this work (Figure 6) for RFCs of at least 10 kW.

TABLE IV.—SUMMARY OF MODELED AND DEMONSTRATED RFC SYSTEM METRICS

Source	Technology[a]	Nominal power level, kW	Application	Maximum storage pressure, MPa (psia)	Specific mass, W·h/kg	Round-trip efficiency (RTE), percent	Notes
Ref. 18 (1970)	PEM	0.2	72 min FC operation, 22 h EZ operation	1.14 (166)	77	33	Demonstrated. Predicted that 38 percent RTE is possible.
Ref. 7 (1972)	Alkaline	7	59 min light, 35 min dark for orbiting space station	2.07 (300)	20.7	29	Modeled. Suggested improvement to 47 percent RTE may be possible.
Ref. 4 (1984)	Alkaline	10	<2 h cycle duration	2.17 (315)	65.4	61.7	Modeled
Ref. 6 (1991)	PEM	12.5	Lunar	20.68 (3,000)	682	39.5	Modeled
Ref. 8 (2003)	Alkaline	6	Lunar south pole	6.89 to 12.0[b] (1,000 to 1,740)	NA	NA	Modeled
Ref. 2 (2003)	PEM	1	12 h charge, 12 h discharge	13.79 (2,000)	555	34	Modeled
Ref. 3 (2006)	PEM	4	12 h charge, 12 h discharge	1.41 (205)	NA	50	Demonstrated. RTE does not include parasitic loads.
Ref. 32 (2020)	PEM	0.1	No specific duration or environment	1.38 (200)	NA	47.4	Demonstrated. RTE does not include parasitic loads.

[a]PEM is proton exchange membrane.

[b]Electrolyzer (EZ) operated at 0.703 MPa (102 psia), then two-stage compressors to store at higher pressure.

In designing power generation and energy storage systems, it is useful to note points where there are decreasing or few benefits to increasing system scale. It is at such a point where an RFC designer may wish to separate the system into modular blocks to ease packaging and improve reliability. This can be seen throughout this report where the rate of increase in RTE or specific energy diminishes in size as RFC power level increases. For example, in Figure 6 at 10.34 MPa (1,500 psia) the RTE for a 10-kW RFC is 38.1 percent, but it increases to only 39.2 percent at 25 kW and 39.3 percent at 50 kW. Past design studies have selected modular units to meet up to 75 kW of electrical power demands (Ref. 4). If there is minimal mass or efficiency benefit to a 50-kW RFC over a 25-kW unit, two 25-kW units provide at least one level of redundancy with conservatively sized electrochemical stacks. Even better would be five 10-kW units. Wynveen presented a baseline design that consisted of four modular units and recommended focusing on enabling improved reliability as opposed to prioritizing improved performance (Ref. 7). Given the scope of RFC reliability unknowns, multiple parallel RFCs is perhaps the only way to meet 5- to 10-year mission life requirements (Ref. 33). The results demonstrated here indicate that modular RFC units may still be the best option to meet mission requirements.

5.0 Conclusions

To best design regenerative fuel cell (RFC) systems for anticipated NASA lunar equator missions, it is necessary to optimize all possible aspects to maximize round-trip efficiency (RTE). Improving RTE also benefits specific energy, reduces required charge energy, and reduces system mass. For example, a 1-percentage-point improvement in RTE reduces total system mass by nearly 3 percentage points. For RFCs scaled from 0.1 to 50 kW nominal net power output, the parasitic power loads were ranked during fuel cell and electrolyzer operation, and effects were evaluated for various operational setpoints and component design and selection. For a small-scale RFC, such as the 0.1-kW-class unit, the primary parasitic loads are related to reactant storage vessel heating, power management voltage converters, and solenoid valves. As RFC power increases, heating and voltage conversion remain significant, but the valves become less impactful. For fuel cell operation, there is an ideal current density to maximize efficiency that holds for all evaluated RFC scales. Although this value is greatly dependent on stack-specific performance, relatively large fuel cells produce the highest efficiency when operating at low current density, near 100 mA/cm^2 here.

Electrolyzer (EZ) operation was discussed to inform stack design decisions related to operating pressure and load profile. These are influential parameters in the resulting electrolysis efficiency and required charge power. Higher EZ operational pressure most negatively impacts both RFC RTE and specific energy. Thinner EZ membranes benefit efficiency at lower pressures, but the increased reactant crossover at higher pressure must be negated by use of thicker membranes to maximize efficiency. Reduced EZ operational temperature improves efficiency at the expense of increased radiator size. For a given RFC scale, there is an RTE benefit to specifying larger EZs and recharging at higher rates, if the RFC can be coupled with a corresponding power source.

Whenever possible, RFC energy storage systems should be designed in conjunction with the power source and customer. This is particularly necessary in cases where there are specific constraints on total volume or packaging specific components such as radiators and solar arrays. Aligning stack voltages and customer bus voltages can eliminate the significant voltage regulation losses. A final notable RTE impact comes from reactant storage subsystem design. Spherical gas storage vessels benefit RTE by 2 to 4 percentage points and increase specific energy by ~50 percent. Cryogenic reactant storage is shown to diminish RTE to below 15 percent in all cases and is thus not practical for lunar equator RFC applications.

Appendix

The design assumptions presented in Table V form the basis of the regenerative fuel cell (RFC) model inputs used throughout the report, unless evaluating a specific factor discussed in the text such as electrolyzer membrane thickness. This includes mission information (i.e., fuel cell (FC), electrolyzer (EZ), and photovoltaic (PV) array inputs) and reactant storage vessel design information such as that based on American Society of Mechanical Engineers (ASME) code.

TABLE V.—REGENERATIVE FUEL CELL DESIGN ASSUMPTIONS

Input	Value	Units	Explanation
Location	Lunar equator	---	Solar power profile and environmental temperature based on Murchison Crater location.
Mission duration	1	year	Used to estimate leak and vent rate of reactants over time to ensure adequate excess reactant capacity.
Mission case	Best or Worst	---	Lunar day cycle with either the most total available solar energy (Best) or least (Worst).
FC power load profile	Constant or Figure 2 net power profile	---	Baseline case uses Figure 2 profile. All other cases assume constant net power requirement.
Design FC current density	200	mA/cm^2	For sizing required FC active area at nominal gross power output. Provides cell voltage of 0.84 Vdc and 54.5 percent efficiency.
Nominal system potential	28 to 120	Vdc	28 to 36 Vdc FC and EZ stack voltages for RFCs of ≤1 kW. 120 Vdc for all larger RFCs.
FC internal cell temperature	70	°C	Affects reactant crossover calculation, thermodynamic properties, and thermal calculations.
Number of FCs in parallel	1 to 7	---	Additional FCs are assumed if required cell active area is unrealistically large for one stack to produce enough power.
Minimum percentage of daytime with PV-only power generation	60	%	Affects solar power profile. Assuming an unrealistically large PV array can reduce RFC energy storage needs.
Percentage of excess reactant stored in vessels	20	%	---
Storage vessel types	Cylindrical or spherical	---	Steel-lined carbon composite pressure vessels
Number of reactant storage vessels	1	Each	---
Storage vessel design safety factor	6	---	Based on ASME Boiler and Pressure Vessel Code Section VIII—Rules for Construction of Pressure Vessels Division I. UG-27.
Product water storage	NA	---	Ideal-sized (calculated for exact model volume of product water) cylindrical carbon composite pressure vessel.
FC operating pressure	45	psia	---
FC membrane thickness	0.178	mm	---
EZ current density limit	1,000	mA/cm^2	---
Voltage regulation efficiency	NA	----	Unless otherwise noted, input and output voltages assumed to float with stack voltage.

References

1. Kerslake, Thomas W.: Electric Power System Technology Options for Lunar Surface Missions. NASA/TM—2005-213629, 2005. https://ntrs.nasa.gov
2. Barbir, Frano; Dalton, L.; and Molter, T.: Regenerative Fuel Cells for Energy Storage: Efficiency and Weight Trade-Offs. AIAA 2003–5937, 2003.
3. Garcia, Christopher P., et al.: Round Trip Energy Efficiency of NASA Glenn Regenerative Fuel Cell System. NASA/TM—2006-214054, 2006. https://ntrs.nasa.gov
4. Chang, B.J., et al.: Engineering Model System Study for a Regenerative Fuel. NASA CR–174801, 1984. https://ntrs.nasa.gov
5. Klein, M.; and Findl, E.: Hydrogen-Oxygen Electrolytic Regenerative Fuel Cells. NASA CR–54461, 1965. https://ntrs.nasa.gov
6. Harris, D.; Gill, S.; and Wallin, W.: Regenerative Fuel Cell Model for Lunar/Mars Surface Stationary and Mobile Power Systems. AIAA 1991–3620, 1991.
7. Wynveen, R.A.; and Schubert, F.H.: Regenerative Fuel Cell Study. NASA CR–128848, 1972. https://ntrs.nasa.gov
8. Ulleberg, Øystein: The Importance of Control Strategies in PV–Hydrogen Systems. Sol. Energy, vol. 76, nos. 1–3, 2004, pp. 323–329.
9. Khan, Z., et al.: Power System Concepts for the Lunar Outpost: A Review of the Power Generation, Energy Storage, Power Management and Distribution (PMAD) System Requirements and Potential Technologies for Development of the Lunar Outpost. NASA/TM—2006-214248, 2006. https://ntrs.nasa.gov
10. National Aeronautics and Space Administration: Long Duration Lunar Energy Storage and Discharge. Small Business Innovation Research (SBIR) and Small Business Technology Transfer (STTR) solicitation, 2019. https://www.sbir.gov/sbirsearch/detail/1547751 Accessed Nov. 29, 2021.
11. Pappa, Richard; and Kerslake, Tom: Mars Surface Solar Arrays: Part 2 (Power Performance). Future In-Space Operations (FISO) Working Group presentation, Cleveland, OH, 2017. https://ntrs.nasa.gov
12. Guzik, Monica C., et al.: Regenerative Fuel Cell Power Systems for Lunar and Martian Surface Exploration. AIAA 2017–5368, 2017.
13. Gilligan, R., et al.: Thermal Design for Extra-Terrestrial Regenerative Fuel Cell System. Presented at the Thermal and Fluids Analysis Workshop, Huntsville, AL, 2017.
14. Gilligan, R., et al.: GT SUITE Fuel Cell Model Validation With Power Module Test Data. Presented at the Thermal and Fluids Analysis Workshop, Galveston, TX, 2018.
15. Gilligan, Ryan P., et al.: Structural Dynamic Testing Results for Air-Independent Proton Exchange Membrane (PEM) Fuel Cell Technologies for Space Applications. IMECE2019–11691, 2019.
16. Guzik, Monica C., et al.: Energy Storage for Lunar Surface Exploration. AIAA 2018–5106, 2018.
17. Burke, Kenneth A.: Unitized Regenerative Fuel Cell System Development. NASA/TM—2003-212739, 2003. https://ntrs.nasa.gov
18. Titterington, William A.: Regenerative Fuel Cell System. AFAPL–TR–70–53, 1970.
19. Brown, Royce, N.: Basic Relationships. Compressors (Third Edition), Ch. 2, Gulf Professional Publishing, Oxford, 2005, pp. 17–51. https://www.sciencedirect.com/science/article/pii/B9780750675451500043 Accessed Nov. 29, 2021.
20. Simons, Sarah, et al.: Novel Concepts and Research. Compression Machinery for Oil and Gas, Klaus Brun and Rainer Kurz, Ch. 16, Gulf Professional Publishing, Oxford, pp. 569–592. https://www.sciencedirect.com/science/article/pii/B978012814683500016X Accessed Nov. 29, 2021.

21. Barbir, F.; Molter, T.; and Dalton, L.: Efficiency and Weight Trade-Off Analysis of Regenerative Fuel Cells as Energy Storage for Aerospace. Int. J. Hydrog., vol. 30, no. 4, 2005, pp. 351–357.
22. Bi, Wu; and Fuller, Thomas F.: Temperature Effects on PEM Fuel Cell Pt/C Catalyst Degradation. ECS Trans., vol. 11, no. 1, 2007, pp. 1235–1246.
23. Shao, Yuyan, et al.: Proton Exchange Membrane Fuel Cell From Low Temperature to High Temperature: Material Challenges. J. Power Sources, vol. 167, no. 2, 2007, pp. 235–242.
24. Zhang, Caizhi, et al.: Determination of the Optimal Operating Temperature Range for High Temperature PEM Fuel Cell Considering Its Performance, CO Tolerance and Degradation. Energy Convers. Manag., vol. 105, 2015, pp. 433–441.
25. Javier Pinar, F., et al.: Effect of Idling Temperature on High Temperature Polymer Electrolyte Membrane Fuel Cell Degradation Under Simulated Start/Stop Cycling Conditions. Int. J. Hydrog., vol. 41, no. 42, 2016, pp. 19463–19474.
26. Levy, Alexander; Van Dine, Leslie L.; and Stedman, James K.: Regenerative Fuel Cell Study for Satellites in GEO Orbit. NASA CR–179609, 1987. https://ntrs.nasa.gov
27. Mittelsteadt, Cortney, et al.: Dimensionally Stable High Performance Membranes. U.S. Department of Energy presentation, 2014. https://www.hydrogen.energy.gov/pdfs/review14/fc036_mittelsteadt_2014_p.pdf Accessed Nov. 29, 2021.
28. Shirvanian, Paige; and van Berkel, Frans: Novel Components in Proton Exchange Membrane (PEM) Water Electrolyzers (PEMWE): Status, Challenges and Future Needs. A Mini Review. Electrochem. Commun., vol. 114, no. 106704, 2020.
29. Smith, Phillip J., et al.: Effect of Reactant Pressure on Proton Exchange Membrane Fuel Cell Performance. NASA/TP-20205011192, 2021. https://ntrs.nasa.gov
30. Smith, Phillip J., et al.: Effect of Reactant Purity on Proton Exchange Membrane Fuel Cell Performance. NASA/TP-20205011711, 2021. https://ntrs.nasa.gov
31. Kenney, Barbara H.; Cull, Ronald C.; and Kankam, M. David: An Analysis of Space Power System Masses. NASA Technical Memorandum 103199, 1990. https://ntrs.nasa.gov
32. Bennett, William R.; Smith, Phillip J.; and Jakupca Ian J.: Analysis of 100-W Regenerative Fuel Cell Demonstration. NASA/TM—20205000357, 2020. https://ntrs.nasa.gov
33. Bents, David J.: Lunar Regenerative Fuel Cell (RFC) Reliability Testing for Assured Mission Success. NASA/TM—2009-215502, 2009. https://ntrs.nasa.gov